THE NOVELTY AND SURFACE-TO-VOLUME-RATIO DEPENDENT ELECTRON BAND STRUCTURE IN SEMICONDUCTOR NANOWIRE

YAO DONGLAI

(Master of Science)

A THESIS SUBMITTED

FOR THE DEGREE OF

DOCTOR OF PHILOSOPHY

DEPARTMENT OF PHYSICS

NATIONAL UNIVERSITY OF SINGAPORE

2011

THE NOVELTY AND SURFACE-TO-VOLUME-RATIO DEPENDENT ELECTRON BAND STRUCTURE IN SEMICONDUCTOR NANOWIRE

YAO DONGLAI

2011

Acknowledgement

This thesis summarizes my research work that has been done since I came to Professor Li Baowen's group in 2006. During my PhD study, I have worked with quite a lot of people whose contribution in assorted ways to the research and the making of this thesis deserved special mention. It is my pleasure to show my gratitude to them all in my humble acknowledgment.

In the first place I would like to record my gratitude to Li Baowen for his supervision, advice, and guidance from the very early stage of this research as well as giving me extraordinary experiences through out the work. Above all and the most needed, he provided me unflinching encouragement and support in various ways. Anytime I was in confusion or lost direction in my study, he will rectify my mistake and guide me to the right way. His truly scientist intuition has made him as a constant oasis of ideas and passions in science, which exceptionally inspire and enrich my growth as a student and a researcher. I also thank him for giving me continuous support and help on applying NUS research scholarship and President Graduates Fellowship, China Overseas Excellent Graduates Awards, Research Assistant position in National University of Singapore and IME Astar Singapore, which support me

from the very base during my whole candidature of my PhD. Without him, I can never reach here. I thank him from my deep heart.

I gratefully acknowledge Professor Zhang Gang, my co-supervisor, for his advice, supervision, and crucial contribution, which made him a backbone of this research and so to this thesis. His involvement with his originality has triggered and nourished my intellectual maturity that I will benefit from, for a long time to come. Professor Zhang, I am grateful in every possible way and hope to keep up our collaboration in the future. Furthermore, I thank him for using his precious times to read this thesis and gave his critical comments about it. I am indebted to him more than he knows.

Many thanks go in particular to Professor Wang Jian-sheng, Professor Gong Jiangbin. I am much appreciated for their valuable advice in science discussion, supervision in courses of computational physics, advanced quantum dynamics. I have also benefited by advice and guidance from Porfessor Wang, who also kindly grants me his time even for answering some of my unintelligent questions.

I would like to thank Department of Physics, Centre for Computation Physics

in National University of Singapore (NUS). It is them who provide me such a good research environment and financial support. A lot of thanks go to Dr. Zhang Xinhuai and Shin Gen, who gives me a lot of help on the high performance computing in SVU and CCSE in NUS.

I also benefited a lot from Professor Li Zhenya, Professor Gao Lei, Professor Shen Mingrong, Professor Jiang Qin, Professor Wu Yinzhong, Professor Zhu Shiqun, Professor Gu Jihua, Professor Gan Zhaoqiang, Professor Nin Zhaoyuan, Professor Fang Liang, Professor Mu Xiaoyong and President Zhu Xiulin during my bachelor and master study in Suzhou University. I specially thank Professor Li Zhenya for his mentorship during my master degree, and Professor Gao Lei for his recommendation to NUS. Many thanks go to Professor Guo Guangyu in National Taiwan University for his patient explanation and detailed instructions on my very first step in the field of ab-init computational physics.

To all the group member: Wang Lei, Wu Gang, Lan Jinhua, Li Nianbei, Yang Nuo, Wu Xiang, Chen Jie, Zhang Lifa, Ren Jie, Shi Lihong, Ni Xiaoxi, Zhang Kaiwen, Xie Rongguo, Xu Xiangfang, Zhu Guimei, Zhang Xun, Ma Jing, Feng Lin, I thank you so much for your useful discussion, sincere comments,

and instructive suggestions not only in the weekly group meeting but also in our personal conversation. I am proud to record that I had several years to work with you all.

Where would I be without my family? My parents deserve special mention for their inseparable support. My mother, Yu Huiyu, in the first place is the person who put the fundament my learning character, showing me the joy of intellectual pursuit ever since I was a child. My father, Yao Huaxiang, is the one who sincerely raised me with his caring and gently love.

Words fail me to express my appreciation to my wife, Hu Wei, whose dedication, love and persistent confidence in me, has taken the load off my shoulder. I owe her for being unselfishly let her intelligence, passions, and ambitions collide with mine. Therefore, I would also thank my parents in-law for letting me take her hand in marriage, and accepting me as a member of the family, warmly.

Finally, I would like to thank everybody who was important to the successful realization of thesis, as well as expressing my apology that I could not mention personally one by one.

Table of Content

ABSTRACT

THE NOVELTY AND SURFACE-TO-VOLUME-RATIO DEPENDENT ELECTRON BAND STRUCTURE IN SEMICONDUCTOR NANOWIRE

By Donglai Yao

In the field of nanotechnology, we focus this thesis on the novelty and surface-to-volume ratio dependent electronic band structure in semiconductor nanowires by means of first principle calculation. Silicon nanowires (SiNWs) in [110] growth direction is main research object, whose cross-sectional geometrics and surface-to-volume ratio dependence on the electronic band gap, effective mass are covered in this thesis. We have found that there is a universal band gap expression which is only related to surface-to-volume ratio for nanowires with dimension up to 7 nm. Most interestingly, this expression is a linear dependence of band gap on surface-to-volume ratio, which is independent of the specific cross sectional shape. We also explore the electron effective mass of [110] silicon nanowires with different cross sectional shapes. We found that the electron effective mass decreases with the SiNW transverse dimension (cross sectional area) increases. With the same cross sectional area,

the triangular cross section SiNW has larger electron effective mass than that of rectangular cross section SiNW. We also trying to find the direct to indirect band gap transition in [110] SiNWs. We successfully estimated the critical dimension where this direct-indirect band gap transition takes place by using the gauge of SVR and the DFT calculation results. It is found that tri-SiNW has the largest transition dimension up to 14 nm in diameter.

Publication List:

1. A Universal Band Gap Expression for Silicon Nanowires of Different Cross-Sectional Geometries, **Donglai Yao**, Gang Zhang, and Baowen Li, **Nano Letters**, 2008, 8 (12), 4557-4561

2. Impacts of Cross-Sectional Shape and Size on Electron Effective Mass of Silicon Nanowires, **Donglai Yao**, Gang Zhang, Guo-Qiang Lo and Baowen Li, **Applied Physics Letters**, **94**, 113113, 2009

3. Size dependent thermoelectric properties of silicon nanowires, Lihong Shi, **Donglai Yao**, Gang Zhang, Baowen Li, **Applied Physics Letters**, **95**, 063102, 2009

4. Large Thermoelectric Figure of Merit In Si1-xGex Nanowires Lihong Shi, **Donglai Yao**, Gang Zhang, Baowen Li, **Accepted** for publication on **Applied Physics Letters**, **2010**

5. Direct to Indirect Band Gap Transition in [110] Silicon Nanowires, **Donglai Yao**, Gang Zhang, and Baowen Li, submitted

LIST OF TABLES

Table:

LIST OF FIGURES

Figures:

Chapter 1

Introduction

1.1 General background from nanotechnology to silicon nanowires.

Nanotechnology is defined as the field of science and technology devoted to studies of the synthesis, properties and applications for structures and materials with at least one critical dimension less than the scale of approximately 100 nm [1] Nanotechnology is the ability to manipulate individual atoms and molecules to produce nanostructured materials and submicron objects that have applications in the real world. Nanotechnology involves the production and application of physical, chemical and biological systems at scales ranging from individual atoms or molecules to about 100 nanometers, as well as the integration of resulting nanostrucures into lager systems. Nanotechology is likely to have a profound impact on our economy and society in the early 21st century, perhaps comparable to that of information technology or cellular and molecular biology. [2] Science and

technology research in nanotechnology promises breakthroughs in areas such as materials and manufacturing, nanoelectronics, medicine and healthcare, energy, biotechnology, information technology and national security. It is widely felt that nanotechnology will be the next industrial revolution.

Nanowires are attracting much interest from those seeking to apply nanotechnology and (especially) those investigating nanoscience. Nanowires, unlike other low-dimensional systems, have two quantum-confined directions but one unconfined direction available for electrical conduction. This allows nanowires to be used in applications where electrical conduction, rather than tunneling transport, is required. Because of their unique density of electronic states, in the limit of small diameters nanowires are expected to exhibit significantly different optical electrical and magnetic properties to their bulk 3-D crystalline counterparts. Increased surface area, very high density of electronic stats and joint density of states near the energies of their van Hove singularities, enhanced exiton binding energy, diameter-dependent band gap, and increased surface scattering for electrons and phonons are just some of the ways in which nanowires different from their corresponding bulk materials. Yet the sizes of nanowires are typically large enough (>1nm(~2 x Si-Si Bond) in the quantum-confined direction) to result in local crystal structures that are

closely related to their parent materials, allowing theoretical predictions about their properties to be made based on knowledge of their bulk prosperities. Not only do nanowires exhibit many properties that are similar to, and others that are distinctly different from, those of their bulk counterparts, nanowires also have the advantage from an applications standpoint in that some of the materials parameters critical for certain properties can be independently controlled in nanowires but no in their bulk counterparts. Certain properties can also be enhanced nonlinearly in small-diameter nanowires, by exploiting the singular aspects of the 1-D electronic density of stats. Furthermore, nanowires have been shown to provide a promising framework for applying the "bottom-up" approach to design of nanostructures for nanoscience investigations and for potential nanotechnology applications.

1.2 Literature reviews.

In "Nanowire Nanosensor for Highly Sensitive and Selective Detection of biological and Chemical Species", Cui et al.[3] reported their fundamental work in the interdisciplinary field of nanowire biosensor. They use the boron-doped silicon nanowires (SiNW) as the highly sensitive, real-time electrically based sensors for biological and chemical species. They noted that

nanowire (NW) and nanotube (NT) can be regarded as possible two candidates of the nano-scale biosensors. They prefer SiNW because silicon does have a well established industrial base, and the dopant type and concentration of SiNW can be well controlled. In addition, the massive existing knowledge of chemical modification of oxide surfaces about SiNW can be exploited.

Bent et al. examined the reaction of the Si(100)-2x1 surface with five-membered cyclic amines. They find out that the connection between Si(100)-2x1 surface and organic molecules could be N-Si bond based on the N-H dissociation. From their work, we can learn that not only the C-Si bond could be formed at the Si surface, but also the N-Si bond. This give us a new idea that we can attach the chemical functional groups, such as amino acid (with N-H bond), as the linking molecules to the SiNW.[4]

In Ref. [5], N. Lorente, et al. studied the SiNW grown along the <100> direction with a bulk Si Core using the density-functional calculations. They found two kinds of surface reconstructions appear with energetical equivalence. One of the reconstructions is found to be strongly metallic while the other one is semimetallic. These results show us that doping is not required in order to obtain good conducting Si nanowire. As we stated above in the

introduction part, it is one of our research interests: the effect of the surface reconstruction.

Ponomareva et al. [6, 7] studied the structure stability, electronic properties and quantum conductivity of small-diameter silicon nanowires. In their papers, they studied quite a few different Silicon Nanowire structures with diameters ranging from 1 to 6nm using the GTBMD scheme [8]. The different growth directions ([111], [110], and [100]) of the nanowire are also investigated. They found that the tetrahedral type nanowires oriented in the <111> direction are the most stable. They also found that the cage-like nanowires have better electrical conducting properties. Getting these results, we have the ideas that the contributions of the surface energy play an important role in the stable nanowire structure.

In Ref. [9], Rurali et al. gives us a detailed report on the size effects in surface-reconstructed <100> and <110> silicon nanowires. They performed ab-init calculation on the electronic structure to study the surface reconstructions of <100> and <110> nanowires with different diameters. The diameter of the small size nanowire is another important factor to influence the band-structure and electronic structure of the nanowire.

1.3 Introduction to our work

Extensive investigations have been carried out on the synthesis, properties and applications of SiNWs. Experimental technology has been developed to control the growth of SiNWs not only in various growth orientations, but also with various shapes of transverse cross section including rectangle (square), hexagon (rough circle), and triangle.[10-14] A large number of theoretical and experimental works have been done to explore the effect of chemical passivation, surface reconstruction, and growth orientations on electronic structures. [11, 15-20] However, compared with the study of these impacts on electronic properties of SiNWs, much less has been done on the impacts of cross sectional geometries. Focusing on the effect of the cross sectional geometries, we have present our research result on this area in Chapter 3.

As the size of the materials is reduced to nanometer regime, the physical and chemical properties of nano scale materials can be significantly changed. One-dimensional systems, such as nanowires and nanotubes are of outstanding current interest as one of the promising building blocks for future nanoscale electronic, optoelectronic, and phononic devices. As the demands of more compact devices emerge, silicon nanowires (SiNWs) have attracted extensive

attention due to their compatibility with Si-based electronic technology. The fascinating potential applications [21] such as novel power device [22], thermoelectric materials [23-26] and, biological and mechanical sensors [27, 28] have attracted wide research interests in recently years. Inspired by experimental works, more and more theoretical efforts have been made to understand the electronic properties of SiNWs. The impacts of the diameter, surfaces reconstruction, and doping have been reported. [23-29] Further developments of SiNW device design require theoretical tools that can provide reasonable quantitative predictions for realistic structures both accurately and time saving. This is hard to achieve with *ab initio* calculations which can only be applied to systems of limited size. One possible way of improving this situation is to use semi-empirical approach such as single band effective mass approximation, which can handle much larger systems.

It is well known that the ultimate speed of integrated circuits depends on the carrier mobility, which is inversely proportional to the effective mass. So the concept of effective mass plays a key role in nanoscale electronics and photonics device design. It has been found that the effective mass of SiNW increases as the transverse dimension decreases, [30] and the effective mass can also be modified by uniaxial strain. [31] Applying strain is a useful

method to modulate band structures and enhance the device performance. It is also a very economical way and has the advantage of being compatible with current CMOS process. The strain can be experimentally realized through depositing a capping layer around the SiNW. At the interface between NW core and the cover layer, the lattice constant mismatch couples to the electronic as well as the optical properties of such system. So it is indispensable to accurately evaluate surface lattice constant of SiNWs. Although some research has been done, many important and fundamental questions remain unsolved. For example, what is the quantum confinement effect on surface lattice constant? And how does the surface lattice constant and electron effective mass depend on nanowire cross-sectional shape? This will be answered in Chapter 4.

Recently, SiNWs attract considerable attention for energy harvesting applications, such as solar cell, due to their unique optical and electrical characteristics. The good absorption for solar energy using SiNW arrays has been demonstrated experimentally and theoretically. [32-34] It is well known that bulk silicon has an indirect band gap, with the valence-band-maximum (VBM) locates at the Γ point and the conduction-band-mimimum (CBM) locates approximately 85% from Γ to X. The indirect band gap characteristic

limits the application of silicon in optoelectrics. However, it is demonstrated both experimentally [35, 36] and theoretically [37, 38] that ultra-thin (1.3 nm in diameter) hydrogen-terminated [110] and [111] SiNW are direct band gap semiconductors. The fundamental band gap characteristic is key role in many applications, such as light emission and absorption. It is indicated the possibility of fabricating Si-based visible optical devices.

Obviously, there exists indirect to direct band gap transition. Using first-principles calculations, it has been shown that the indirect-to-direct energy gap transition for [111] SiNWs at a diameter of less than 2.2 nm. [37] However, the situation with [110] SiNW is still unknown, which wires seem to be the most promise candidate for the nanowires electronic device and bio-sensor because the band gaps of [110] SiNWs is the smallest among those of the [100], [112] and [111] wires of the same diameter [39]. Moreover, so far there is no systematic report on the indirect-direct band gap transition, and its dependence on the geometry of SiNWs. As the indirect band gap and consequential weak light absorption remain the bottleneck for their application in optoelectronics/solar PV, a detailed understanding of the indirect-to-direct band transition via diameter is of primary importance to the development of new applications for SiNWs. It could be extremely difficult to get this information from experiments. In Chapter 5, we studied the direct to indirect

band gap transition when the transverse cross section of SiNW is increased, by using first-principle calculations. An extremely linear dependence on the surface-to-volume ratio is found for both the lowest and second-lowest conduction band edge.

References:

[1]. F. Patolsky, G. Zheng, and C. M. Lieber, Nanomedicine 1, 51 (2006).

[2]. Handbook of Nanotechnology, Bhushan, Springer.

[3] Y. Cui et al., Science 293, 1289 (2001).

[4] G. T. Wang, and S. F. Bent, Journal of Physical Chemistry B 107, 4982 (2003).

[5] R. Rurali, and N. Lorente, Physical Review Letters 94, 026805 (2005).

[6] I. Ponomareva et al., Physical Review Letters 95, 265502 (2005).

[7] I. Ponomareva et al., Physical Review B 74, 125311 (2006).

[8] M. Menon, and K. R. Subbaswamy, Physical Review B 55, 9231 (1997).

[9] R. Rurali, A. Poissier, and N. Lorente, Physical Review B 74, 165324 (2006).

[10] Duan, X. F.; Huang, Y.; Cui, Y.; Wang, J. F.; Lieber, C. M. *Nature* **2001,** *409*, 66.

[11] Ma, D. D. D.; Lee, C. S.; Au, F. C. K.; Tong, S. Y.; Lee, S. T. *Science* **2003,** *299*, 1874.

[12] Zhang, R. Q.; Lifshitz, Y.; Lee, S. T. *Advanced Materials* **2003,** *15*, 635.

[13] Friedman, R. S.; McAlpine, M. C.; Ricketts, D. S.; Ham, D.; Lieber, C. M. *Nature* **2005,** *434*, 1085.

[14] Sirbuly, D. J.; Law, M.; Yan, H. Q.; Yang, P. D. *Journal of Physical Chemistry B* **2005,** *109*, 15190.

[15] Fernandez-Serra, M.-V.; Hadéis, Ch.; and Blase, X. Nano Letters, **2006**, *6*, 2674.

[16] Rurali, R.; and Lorente, N. Phys. Rev. Lett., **2005**, *94*, 026805.

[17] Ng, M.-F.; Zhou, L.; Yang, S.-W.; Sim, L. Y.; Tan, V. B. C.; and Wu, P. Phys. Rev. B, **2007**, *76*, 155435.

[18] Yan, J. A.; Yang, L.; Chou, M. Y. *Physical Review B* **2007,** *76*, 115319.

[19] Vo, T.; Williamson, A. J.; Galli, G. *Physical Review B* **2006,** *74*, 045116.

[20] Nolan, M.; O'Callaghan, S.; Fagas, G.; and Greer, J. C. *Nano Letters* **2007**, 7, 34.

[21] Y. Li, F. Qiang, J. Xiang, C. M. Lieber, Materials Today **9**, 18 (2006).

[22] B. Tian, X. Zheng, T. J. Kempa, Y. Fang, N. Yu, G. Yu, J. Huang, C. M. Lieber, Nature **449**, 885 (2007).

[23] T. T. M. Vo, A. J. Williamson, V. Lordi, G. Galli, Nano Lett. **8**, 1111 (2008).

[24] A. I. Hochbaum, R. Chen, R. D. Delgado, W. Liang, E. C. Garnett, M. Najarian, A. Majumdar, P. D. Yang, Nature **451**, 163 (2008).

[25] A. I. Boukai, Y. Bunimovich, J. Tahir-Kheli, J.-K. Yu, W. A. Goddard III, J. R. Heath, Nature **451**, 168 (2008).

[26] N. Yang, G. Zhang, B. W. Li, Nano Lett. **8**, 276 (2008).

[27] Y. Cui, Q. Q. Wei, H. K. Park, C. M. Lieber, Science **293**, 1289 (2001).

[28] Y. Cui, C. M. Lieber, Science **291**, 851 (2001).

[29] T. Vo, A. J. Williamson, G. Galli, Phys. Rev. B **74**, 045116 (2006).

[30] E. Gnani, S. Reggiani, A. Gnudi, P. Parruccini, R. Colle, M. Rudan, G. Baccarani, IEEE Transactions On Electron Devices **54**, 2243 (2007).

[31] D. Shiri, Y. Kong, A. Buin, M. Anantram, Appl. Phys. Lett. **93**, 073114 (2008).

[32] B. M. Kayes, H. A. Atwater, N. S. Lewis, J. Appl. Phys. **97**, 114302, (2005).

[33] L. Hu, G. Chen, Nano Lett. **7**, 3249 (2007).

[34] J. S. Li, H. Y. Yu, S. M. Wong, G. Zhang, X. W. Sun, G. Q. Lo, D. L. Kwong, Appl. Phys. Lett., **95**, 033102 (2009).

[35] Y. Cui, Z. H. Zhong, D. L. Wang, W. U. Wang, C. M. Lieber, Nano Lett. **3**, 149 (2003).

[36] D. D. D. Ma, C. S. Lee, F. C. K. Au, S. Y. Tong, S. T. Lee, Science **299**, 1874 (2003).

[37] X. Y. Zhao, C. M. Wei, L. Yang, M. Y. Chou, Phys. Rev. Lett. **92**, 236805 (2004).

[38] K.-H. Hong, J. Kim, S.-H. Lee, J. K. Shin, Nano Lett. **5**, 1335 (2008).

[39] R. Q. Zhang, Y. Lifshitz, S. T. Lee, Adv. Mater. **15**, 635 (2003).

Chapter 2

Modeling and Methodology

This chapter is concerned with the basic physical description of electrons in nanowires. Two atomistic methods have been applied in this thesis: Density functional theory (DFT) and Density Functional based Tight-Binding (DFTB).

2.1 Density Functional Theory

DFT is the most widely used method for electronic structure calculations in condensed matters. Being an *ab initio* method, no fitting parameters are needed, and DFT is thus very powerful in the research of novel materials, including nano-structured systems. With present day computer resources, systems sizes of O(1000) atoms can be studied within standard DFT.

2.1.1 The many body problem

The starting point in the description of a system containing electrons and

nuclei is the Hamiltonian

$$\hat{H} = -\frac{\hbar^2}{2m_e}\sum_i \nabla_i^2 - \sum_{i,I}\frac{z_I e^2}{|r_i - R_I|} + \frac{1}{2}\sum_{i\neq j}\frac{e^2}{|r_i - r_j|}$$
$$-\sum_I \frac{\hbar^2}{2M_I}\nabla_I^2 + \frac{1}{2}\sum_{I\neq J}\frac{Z_I Z_J e^2}{|R_I - R_J|} \quad (2.1)$$

where lower case subscripts denote electrons, and upper case subscripts denotes nuclei. Z_I and M_I are the charge and mass of the nuclei. The inverse of the nuclei masses, $1/M_I$, can be regarded as such small quantities that the nuclei kinetic energy can be ignored. Alternatively, one can argue that the large difference in mass between the electrons and the nuclei effectively means that electrons react almost instantaneously to changes in the nuclei positions, and the nuclei can be regarded as static. This is the so-called Born-Oppenheimer approximation. The relevant Hamiltonian for electronic structure calculations is thus

$$\hat{H} = \hat{T} + \hat{V}_{ext} + \hat{V}_{int} + E_{II}, \quad (2.2)$$

where $\hat{T} = -\frac{1}{2}\sum_i \nabla_i^2$ is the kinetic energy operator for electrons, $\hat{V}_{ext} = -\sum_{i,I}\frac{z_I e^2}{|r_i - R_I|}$ is the potential due to the nuclei, and $\hat{V}_{int} = \frac{1}{2}\sum_{i\neq j}\frac{e^2}{|r_i - r_j|}$ is the internal electron-electron interaction. E_{II} is the constant energy of the nucleus-nucleus interactions. The Hamiltonian (2.2) is uniquely determined by the external potential, $\hat{V}_{ext}$, (which also determines E_{II}) since $\hat{T}$and $\hat{V}_{int}$ are the same for any N electron problem. The properties of the interacting system

with N electrons are in principle obtainable from the

time-independent Schrodinger equation:

$$\widehat{H}\Psi_i(\boldsymbol{r}_1, \boldsymbol{r}_2 \dots, \boldsymbol{r}_n) = E_i\Psi_i(\boldsymbol{r}_1, \boldsymbol{r}_2 \dots, \boldsymbol{r}_n). \quad (2.3)$$

Solving Eq. (2.3) for a realistic system containing many electrons and nuclei is in general an intractable task due to 'the exponential wall' [1] – the memory needed to describe a state, $\Psi_i(\boldsymbol{r}_1, \boldsymbol{r}_2 \dots, \boldsymbol{r}_n)$, of $3N$ variables grows exponentially as p^{3N}, with $p \geq 3$ being some integer number of interpolation points needed to describe the wave function in one variable.

2.1.2 Density functional theory

The theoretical foundation of DFT was made by Hohenberg and Kohn [2] who showed that there is a one-to-one correspondence between the ground state density of a system and the external potential. In other words, two external potentials differing by more than a constant lead to two different ground state densities. Since the Hamiltonian (2.2) is uniquely determined by the external potential, it follows that all properties, including exited states, of the system can be regarded as functionals of the ground state density. Specifically, the total energy can be considered as a functional of the density:

$$E[n] = T[n] + V_{int}[n] + V_{ext}[n] = T[n] + V_{int}[n] + \int d\boldsymbol{r} n(\boldsymbol{r}) v_{ext}(\boldsymbol{r}), \quad (2.4)$$

The minimum energy is found for the ground state density, n_0, which can be shown by the variational principle.

Considering the three-dimensional density instead of the 3*N*-dimensional wave vectors as the independent variable is a huge simplification, however the progress is still mostly formal. The problem is that the universal functional *T[n]* and $V_{int}[n]$ of the kinetic and electron-electron interaction energies are unknown.

2.1.3 Kohn-Sham equations

Almost any practical use of DFT rely on the work of Kohn and Sham (KS) [Ref. A64]. KS theory rely on a basic ansatz, namely that any ground state density, *n(r)*, of an interacting system, is also the ground state density of a non-interacting system with an effective potential, $V_{eff}(r)$:

$$\widehat{H}_{KS} = -\frac{1}{2}\nabla^2 + \mathrm{V_{eff}}(\mathbf{r}) \quad (2.5)$$

Furthermore, the KS approach splits up the energy contributions into known and 'easy' parts which give the main contributions to the total energy, and unknown and 'difficult' parts which are accounted for by suitable

approximations.

Specifically, the kinetic energy $T[n]$ is split in two: $T[n] = T_s[n] + T_c[n]$, where $T_s[n] = T_s[\{\phi_i[n]\}] = -\frac{1}{2}\sum_i^N \int d\boldsymbol{r}\phi_i(\boldsymbol{r})^*\nabla^2\,\phi_i(\boldsymbol{r})$ is the kinetic energy of non- interacting particles, with $n = \sum_i^N|\phi_i(\boldsymbol{r})|^2$. The remaining of the interacting kinetic energy, $T_c[n]$, is called correlation and is included by suitable approximations. Similarly, the electron-electron interaction energy is split into a simple and complicated part: $V_{int}[n] = V_H[n] + V_x[n] + V_c[n]$, where the Hartree term is $V_H[n]$. The remaining parts are the exchange energy $V_x[n]$ which is a repulsive term due to the Pauli exclusion principle, and the correlation term $V_c[n]$ which is due to electron-electron correlations not captured in the Hartree term. The latter two terms are, like $T_c[n]$, dealt with by suitable approximations. The KS energy functional is often written as

$$E_{KS}[n] = T_s[\{\phi_i[n]\}] + V_H[n] + E_{xc}[n] + E_{II}, \qquad (2.6)$$

where the exchange-correlation energy, $E_{xc}[n] = T_c[n] + V_x[n] + V_c[n]$. The validity of any KS DFT calculation relies on good approximations of $\boldsymbol{E_{xc}}$. A widely used approximation for $\boldsymbol{E_{xc}}$ is the local density approximation (LDA) where the contribution of each volume element to the total exchange correlation energy is taken to be that of an element of a homogeneous electron gas of the density at that point:

$$E_{xc}^{LDA}[n] = \int d\boldsymbol{r} n(\boldsymbol{r}) \epsilon_{xc}^{hom}[n(\boldsymbol{r})]. \quad (2.7)$$

More elaborate approaches which also take the gradient of the density into account are known as the generalized gradient approximation (GGA), which will be applied in Chapter 4.

In order to actually calculate the ground state density, the KS equations must be solved self-consistently:

$$\left[-\frac{1}{2m_e}\nabla^2 + V_{\text{eff}}(\boldsymbol{r})\right]\psi_i(\boldsymbol{r}) = \epsilon_i \psi_i(\boldsymbol{r}), \quad (2.8)$$

$$V_{\text{eff}}(\boldsymbol{r}) = \int \mathrm{d}\mathbf{r}' \frac{e^2 n(\boldsymbol{r}')}{|\boldsymbol{r}-\boldsymbol{r}'|} + V_{ext}(\boldsymbol{r}) + \frac{\delta E_{xc}[n(\boldsymbol{r})]}{\delta n(\boldsymbol{r})}, \quad (2.9)$$

$$n(\boldsymbol{r}) = \sum_{\boldsymbol{i}} |\psi_i(\boldsymbol{r})|^2 \ , \quad (2.10)$$

The last term in (2.9) is the functional derivative of the exchange-correlation energy, $E_{xc}[n]$.

Summarizing, the problem of minimizing the total energy $E[n]$ given by Eq. (2.4) is replaced by the problem of solving a non-interacting Schrodinger equation self-consistently, Eqs. (2.8) - (2.10), which reproduce the interacting ground state density, $n(\boldsymbol{r})$.

2.2 Tight Binding Method

The tight-binding (TB) method lies between the accurate but expensive DFT methods and the fast, but limited continuum methods such as effective mass and $\boldsymbol{k}\cdot\boldsymbol{p}$ theory. Heterostructures, quantum confinement, atomic disorder and surface roughness can be treated quantitatively with TB but only qualitatively with the continuum models. If computer resources were unlimited, DFT or other *ab initio* methods would be preferable. However, since this is not the case, the major advantage of TB over DFT is that much larger system sizes can be modeled. Quantum dot structures with more than 50 millions atoms have been modeled with the NEMO-3D TB code[3].

In the context of nanowire research, there is at present a size gap between the largest structures manageable with DFT and the typical structures in experiments, D > 10 nm. Tight-binding modeling is one way to abridge this gap, as NWs with diameters =10~20 nm can be modeled using atomistic tight-binding (TB) methods [4]. TB models have been applied to both Si, Ge, and III-VI nanowires [4], and a number of parameterizations are available in the literature. Focusing on Si, the simplest TB description consists of a nearest neighbor sp3 model in which each Si atom has four orbitals (s, p_x, p_y, p_z) [5].

To accurately model the conduction band it is necessary to include either more orbitals (typically five d and one extra s* orbitals) or to include next-nearest neighbor hopping [6].

Structural relaxation can be performed within some TB models using only the electronic structure [7]. However, calculations of structural and energetic properties typically require inclusion of a repulsive energy term that is independent of the electronic structure [8]. In the case of nanowire modeling, structural relaxation is typically not performed, and the focus is solely on the electronic properties of a wire which is simply cut out from a bulk crystal with the atoms held fixed.

Clearly, tight-binding rely on appropriate parameters, and is by no means an ab initio method. However, due to the atomistic description of the bonding, the same set of TB parameters are often applicable to different atomic structures, e.g. diamond-lattice, HCP, BCC [7], or in strained structures [9, 10, 11]. Also, the TB parameters do not depend on the NW orientation. Energetic and scattering properties of vacancies can be modeled by TB. Impurities can be modeled within TB but requires appropriate TB parameters, which only exist for few atomic species. The transferability to nanostructures of such

parameters can be questioned since surface effects such as surface relaxation might be important.

2.3 Density Functional Tight Binding

The Density Functional based Tight Binding method is based on a second-order expansion of the Kohn-Sham total energy in Density-Functional Theory (DFT) with respect to charge density fluctuations. The zeroth order approach is equivalent to a common standard non-self-consistent (TB) scheme, while at second order a transparent, parameter-free, and readily calculable expression for generalized Hamiltonian matrix elements can be derived. These are modified by a self-consistent redistribution of Mulliken charges (SCC).

Besides the usual "band structure" and short-range repulsive terms the final approximate Kohn-Sham energy additionally includes a Coulomb interaction between charge fluctuations. At large distances this accounts for long-range electrostatic forces between two point charges and approximately includes self-interaction contributions of a given atom if the charges are located at one and the same atom. Due to the SCC extension, DFTB can be successfully

applied to problems, where deficiencies within the non-SCC standard TB approach become obvious.

In the last few years, the DFTB method had been heavily extended to allow the calculation of optical and excited state properties. The GW formalism as well as time dependent DFTB had been implemented. Furthermore, DFTB had been used to calculate the Hamiltonian for transport codes, using Green functions techniques.

2.4 DFT applied to Silicon nanowires

Within the last ten years a number of publications have applied DFT calculations to study the electronic and structural properties of ultra-thin SiNWs. The majority of the works use standard DFT within the LDA/GGA approximation and include studies of the energetics of dopant impurities [12, 13, 14, 15], surface passivation [16], surface reconstruction [17], band structure effects vs diameter [3], mechanical properties and phonons [18, 19, 20, 21], and transport [12, 13, 22, 23]. Standard DFT is applicable to systems containing 1000 atoms, thus limiting the nanowire diameter to 3−4 nm for band structure calculations. For transport calculations, where several unit cells need to be included in the DFT super cell, the diameter range is even narrower.

DFT based calculations are particularly useful when modeling systems with different atomic species or with geometries that deviates significantly from the corresponding bulk materials, where TB calculations are insufficient. In the case of NWs such situations include the energetic and scattering properties of doping atoms, surface passivation, or surface reconstruction.

Experimentally produced SiNWs are typically passivated by a thin amorphous SiO_2 surface layer. To our knowledge, few DFT calculations of SiNWs have treated the SiO_2 surface. The standard approach is instead to passivate the surface with H atoms, which guarantees that the SiNW becomes semiconducting. The purpose usually is not to model the Si-H interaction in detail, but only to passivate the Si dangling bonds. In justice, it is important to mention that SiNWs indeed can be H-passivated if the silicon dioxide is removed in a HF etch [24]. It still remains to be investigated what influence the amorphous SiO_2 surface has on the thin NW properties. Going beyond standard DFT, a few studies have calculated the band gap and optical properties of SiNWs using the GW method and time-dependent DFT [25, 26, 27]. The GW band gaps were shown to agree well with experiments. Notably, the GW corrections to the LDA/GGA band gap are larger for the smallest wires due to self-energy corrections not captured in LDA. For the smallest

wires, the self-energy corrections tend to dominate over quantum confinement effects.

2.5 Discussion

The choice of electronic structure model of course depends on the specific questions to be answered. If one is only interested in the qualitative behavior of the band structure close to the band edges, a $\boldsymbol{k}\cdot\boldsymbol{p}$ model will probably often be sufficient. Alternatively, a DFTB/TB model will be adequate for band structure calculations in a relatively large diameter interval. Concerning transport calculations, the DFTB/TB and local orbital DFT approaches seem to be the natural choices, when focus is on specific scattering effects, and one wants to go beyond the Boltzmann transport equation [28] with phenomenological scattering rates. The DFTB/TB model seems adequate for calculating scattering by vacancies and surface roughness, since larger and hence more realistic wires can be studied.

On the other hand, energetics and scattering properties of impurities is most naturally studied with DFT due to the lack of DFTB/TB parameters between Si and the impurity atoms, which further might be dependent on the specific

position of the impurity. In the present thesis, the use of DFTB and DFT methods is primarily considered as an accurate way to find the electronic band structure and band gaps.

References:

[1]. W. Kohn. Nobel lecture: Electronic structure of matter—wave functions and density functionals. Rev. Mod. Phys., 71(5): 1253, 1999

[2]. P. Hohenberg and W. Kohn. Inhomogeneous electron gas. Phys. Rev., 136(3B):B864–B871, 1964

[3]. R. Rurali, B. Aradi, T. Frauenheim, and A. Gali. Electronic structure of semiconductor nanowires. Phys. Rev. B, 76:113303, 2007

[4]. Y. M. Niquet, A. Lherbier, N. H. Quang, M. V. Fern ́andez-Serra, X. Blase, and C. Delerue. Electronic structure of semiconductor nanowires. Phys. Rev. B, 73(16):165319, 2006

[5]. D. J. Chadi. Localized-orbital description of wave functions and energy bands in semiconductors. Phys. Rev. B, 16(8):3572–3578, 1977.

[6]. T. B. Boykin, G. Klimeck, and F. Oyafuso. Valence band effectivemass expressions in the sp3d5s* empirical tight-binding model applied to a Si and Ge parametrization. Phys. Rev. B, 69:115201, 2004.

[7]. N. Bernstein, M. J. Mehl, D. A. Papaconstantopoulos, N. I. Papanicolaou, M. Z. Bazant, and E. Kaxiras. Energetic, vibrational,

and electronic properties of silicon using a nonorthogonal tight-binding model. Phys. Rev. B, 62(7):4477, 2000.

[8]. C. M. Goringe, D. R. Bowler, and E. Hernandez. Tight-binding modelling of materials. Rep. Prog. Phys., 60(12):1447–1512, 1997

[9]. T. B. Boykin, G. Klimeck, R. C. Bowen, and F. Oyafuso. Diagonal parameter shifts due to nearest-neighbor displacements in empirical tight-binding theory. Phys. Rev. B, 66(12):125207, 2002.

[10]. G. Klimeck, S.S. Ahmed, Hansang Bae, N. Kharche, S. Clark, B. Haley, Sunhee Lee, M. Naumov, Hoon Ryu, F. Saied, M. Prada, M. Korkusinski, T.B. Boykin, and R. Rahman. Atomistic simulation of realistically sized nanodevices using nemo 3-d—part i: Models and benchmarks. Electron Devices, IEEE Transactions on, 54(9):2079–2089, Sept. 2007.

[11]. Y. M. Niquet, D. Rideau, C. Tavernier, H. Jaouen, and X. Blase. Onsite matrix elements of the tight-binding hamiltonian of a strained crystal: Application to silicon, germanium, and their alloys. Phys. Rev. B, 79(24):245201, 2009

[12]. M. V. Fernandez-Serra, Ch. Adessi, and X. Blase. Surface segregation and backscattering in doped silicon nanowires. Phys. Rev. Lett., 96:166805, 2006

[13]. M. V. Fernandez-Serra, Ch. Adessi, and X. Blase. Conductance, surface traps, and passivation in doped silicon nanowires. Nano Lett., 6:2674–2678, 2006

[14]. H. Peelaers, B. Partoens, and F.M. Peeters. Formation and segregation energies of b and p doped and bp codoped silicon nanowires. Nano Lett., 6:2781–2784, 2006

[15]. H. Peelaers, B. Partoens, and F. M. Peeters. Properties of b and p doped Ge nanowires. Appl. Phys. Lett., 90(26):263103, 2007

[16]. M. Nolan, S. O'Callaghan, G. Fagas, J. C. Greer, and T. Frauenheim. Silicon nanowire band gap modification. Nano Lett., 7:34–38, 2007

[17]. R. Rurali and N. Lorente. Metallic and semimetallic silicon [100] nanowires. Phys. Rev. Lett., 94:026805, 2005

[18]. P. W. Leu, A. Svizhenko, and K. Cho. Ab initio calculations of the mechanical and electronic properties of strained Si nanowires. Phys. Rev. B, 77:235305, 2008

[19]. K. H. Hong, J. Kim, S.-H. Lee, and J. K. Shin. Strain-driven electronic band structure modulation of Si nanowires. Nano Lett., 8(5):1335–1340, 2008.

[20]. T. Markussen, A.-P. Jauho, and M. Brandbyge. Heat conductance is strongly anisotropic for pristine silicon nanowires. Nano Lett., 8:3771, 2008

[21]. H. Peelaers, B. Partoens, and F. M. Peeters. Phonon band structure of Si nanowires: A stability analysis. Nano Lett., 9(1):107–111, 2009

[22]. T. Markussen, R. Rurali, A.-P. Jauho, and M. Brandbyge. Scaling theory put into practice: First-principles modeling of transport in doped silicon nanowires. Phys. Rev. Lett., 99:076803, 2007

[23]. R. Rurali, T. Markussen, J. Sune, M. Brandbyge, and A.-P. Jauho. Modeling transport in ultrathin Si nanowires: Charged versus neutral impurities. Nano Lett., 8:2825, 2008

[24]. D. D. D. Ma, C. S. Lee, F. K. Au, S. T. Tong, and S. T. Lee. Smalldiameter silicon nanowire surfaces. Science, 299:1874, 2003

[25]. M. Bruno, M. Palummo, A. Marini, R. Del Sole, and S. Ossicini. From Si nanowires to porous silicon: The role of excitonic effects. Phys. Rev. Lett., 98(3):036807, 2007

[26]. X. Zhao, C. M. Wei, L. Yang, and M. Y. Chou. Quantum confinement and electronic properties of silicon nanowires. Phys. Rev. Lett., 92:236805, 2004

[27]. R. He and P. yang. Giant piezoresistance effect in silicon nanowires. Nat. Nano., 1:42, 2006

[28]. D. K. Ferry and S. M. Goodnick. Transport in Nanostructures. Cambridge University Press, 1997

Chapter 3

A Universal Expression of Band Gap for Silicon Nanowires of Different Cross-Section Geometries

In this chapter, we use the first-principles tight binding method to investigate the electronic structure and band gap of [110] oriented hydrogen-passivated silicon nanowires (SiNWs) of different cross sectional geometries. A quantitative universal band gap expression for [110] SiNWs is obtained, which shows a linear dependence of band gap on the surface area to volume ratio (SVR), and it is independent of the cross sectional geometry. In contrast to the ambiguity in the definition of the SiNWs transverse dimension, using of SVR has the advantage to readily predict band gap for SiNWs with any cross sectional shapes. Our results demonstrate that the SVR is an ideal “gauge” to describe the band gap of SiNWs.

3.1 Introduction

Silicon nanowires (SiNWs) are one of the promising building blocks for future nanoscale devices due to their ideal interface compatibility with Si-based electronic technology. Their fascinating potential applications, such as bio-sensor [1,2], thermoelectric materials,[3-6] and power devices [7], have attracted broad interests in recently years. Extensive investigations have been carried out on the synthesis, properties and applications of SiNWs. Experimental technology has been developed to control the growth of SiNWs not only in various growth orientations, but also with various shapes of transverse cross section including rectangle (square), hexagon (rough circle), and triangle.[8-12] A large number of theoretical and experimental works have been done to explore the effect of chemical passivation, surface reconstruction, and growth orientations on electronic structures. [9, 13-18] However, compared with the study of these impacts on electronic properties of SiNWs, much less has been done on the impacts of cross sectional geometries.

3.2 SVR (Surface-to-Volume Ratio)

The surface area to volume ratio (SVR) increases as the system scales down. It thus plays more and more important role when the device becomes smaller and smaller. For

example, materials with high SVR react at much faster rates than monolithic materials. It has also been shown that SVR also affects the physical properties of nano materials remarkably. [18-21] However, the researches so far have been qualitative.

In this chapter, we study *quantitatively and systematically* the impact of SVR on electron band structure of [110] oriented, hydrogen passivated SiNWs. The impacts of cross sectional shapes, including trianglular-, rectangular- and hexagonal-SiNWs are investigated. For simplicity, they are named as tri-SiNWs, rect-SiNWs and hex-SiNWs respectively. We find, for the first time, a general expression for band gaps of SiNWs, which shows linear dependence on SVR, and it is independent of cross sectional shape.

3.3 Density Functional Tight Binding (Methodology)

We focus on SiNWs oriented along the [110] direction since small diameter SiNWs have been observed to grow experimentally mostly along this direction, and it has been demonstrated that [110] is the optimum orientation that offers the highest ON-current and smallest intrinsic device delay for the same OFF-current for SiNW transistors. [17, 22] Moreover, [110] wires seem to be the most sensitive candidate for the nanowires sensor because the band gaps of [110] SiNWs is the smallest among those of the [100], [112] and [111] wires of the same diameter [10]. Figure 3.1 shows the schematic pictures of the SiNWs of different cross section, the transverse size, D is between 1.4 and 7.2 nm. Here

D is defined as the largest distance between the terminating hydrogen atoms in the cross section plane. *D*, the number of atoms per supercell (*N*), and cross sectional area (*A*) of the SiNWs are summarized in Table 3.1. The transverse size, *D*, of SiNWs can be controlled experimentally from 1.3 to 7 nm [9], so the SiNWs we explore here are within the range of the experimental observation.

The tri-, rect-, and hex-SiNWs are the realistic crystalline structures of SiNWs, which have been studied widely [17-27]. For each NW, the atomic structure is initially constructed from diamond structured bulk silicon. The structure of the silicon core of the NWs is constructed by selecting all the Si atoms that fall within a virtual cage placed in bulk silicon while silicon atoms falling outside this virtual cage are removed and the surface dangling bonds were terminated with hydrogen atoms placed at a standard bond length of 1.48 Å that eliminate artificial dangling bonds. This Si-H bond length corresponds to that in SiH_4 molecule. Due to the small dimensions, the surface reconstruction will affect the band structure. [17] Here, we concentrate on the dependence of band structure on the size and transverse cross sectional shapes. Therefore, no surface reconstruction is considered in this study. This H-termination model without surface reconstruction is widely used to study the size effect on electronic structure of SiNWs. [15, 16]. The dimensions and cross sectional shapes of the NWs were varied by changing the virtual cages. The initial geometries are then relaxed to their closest minimum total energy. A supercell approach is adopted where each wire is periodically repeated along

the growth direction [110]. The size of the supercells in the transverse plane is so large as to avoid interaction between the SiNW and its images in neighboring cells (>15 Å from surface to surface). Previous calculations by first principles have been performed to study the electronic structure of SiNWs with diameters less than 3.4 nm. [17, 18, 21] However, the diameters of the wires considered in these studies were too small to study systematically the size effects on band gap. To investigate the electronic properties of SiNWs with diameter up to 7 nm, the density functional derived tight-binding method (DFTB) [28, 29] is used. The DFTB is based on the expansion of the Kohn-Sham density functional in the local density approximation (LDA) to second order over the density fluctuations around a suitable electron density. In contrast to the tight-binding (TB) method, the one- and two-center matrix elements of the associated Hamiltonian are calculated in an explicit minimal valence basis. The repulsive energy part is approximated by universal pair potentials, which are fitted using the data of self-consistent-field LDA calculations. The DFTB has a minimal number of input parameters and retain the efficiency of TB approaches. In contrast to the conventional density functional theory (DFT) methods, the DFTB has higher computational efficiency which means that the DFTB allows the simulation of bigger systems than conventional DFT at a reasonable computational time and achieve similar accuracy. This DFTB scheme has been used to calculate structure and band gap of SiNWs [18, 21] and fullerene [30] successfully. In this work, the structural relaxation is performed using a conjugate gradient method. The

atomic force tolerance of $3x10^{-4}$ eV/Å is applied. Self-consistent charge tolerance is 10^{-5} au. In assessing the accuracy of the computational method, we perform calculations for the Si-Si bond length and band gap on bulk silicon. The calculated Si-Si bond length and band gap for bulk silicon are 2.30 Å and 1.29 eV, respectively, which are close to the experimental values (2.35 Å and 1.17 eV) [31]. In contrast to the underestimated band gaps (up to 0.6 eV) predicted by commonly used DFT methods [16], the band gap calculated by DFTB is very close to the experimental value of 1.17 eV. And as all the Si atoms in SiNWs remain in a closed shell configuration with four nearest neighbors similar to the bulk structure, we anticipate that the DFTB calculations will predict the stable nanowire structures to a similar level of accuracy to that of the bulk structure.

3.4 Results and Discussion

After the optimized structures for these SiNWs are obtained, we figure out the band structures for the SiNWs. In Figs. 3.2-3.4 the electron band structures of NWs with different cross sections are compared. The band structures are shown along the growth direction of the wires. The band structures corresponding to the three cross sectional shapes reveal that for [110] SiNWs, all the band gaps are direct. Here we only show the band structures of SiNWs with transverse dimensions of about 1nm and 3 nm, as the band structures of larger SiNWs are similar. The band structures are generally consistent to

those calculated by first principles methods. [16, 17] It is well known that bulk silicon has an indirect band gap, with the valence-band-maximum (VBM) locates at the Γ point and the conduction-band-mimimum (CBM) locates approximately 85% from Γ to X. With the dimensions of silicon are reduced from the bulk to nano scale, quantum confinement effect increases the energy of CBM and decreases the energy edge of the VBM, and increases the band gap of the system. This quantum confinement effect is obvious in Figs. 3.2-3.4. However, the magnitude of the energy increase/decrease induced by quantum confinement is different for each point in the band structure. It is predicted that the CBM energy increases more near the X point than near Γ. Therefore, for nanostructured wires with sufficiently small dimensions, this difference in energy shifts at different points in the Brillouin zone is large enough to move the CBM at the X point above the CBM at the Γ point. [17] Then a transition from an indirect to direct gap material occurs. Our results show that in [110] SiNWs, the indirect to direct transition does not depend on the special cross sectional shapes. And the band gaps of [110] SiNWs remain direct even for SiNWs with dimensions up to 7 nm.

Having discussed the direct nature of the band gap, we now turn to the magnitude of the band gaps. The dependence of band gap on SiNW dimension D is shown in Fig. 3.5a. It is obvious that the smaller the dimension of the wire the larger the band gap due to quantum confinement. As D decreases from 7 nm to 1 nm, the band gap increases from 1.5 eV to 2.7 eV. In addition to the size dependence, the most interesting feature we

should like to point out is that the energy gap also shows significantly different change with respect to the cross sectional shape. The band gaps of rect- and hex-SiNWs are rather close, while distinctly smaller than that for the tri-SiNWs. The band gaps of [110] SiNWs with different cross sectional patterns were investigated by Ng *et al.* [15] In their calculations, additional hexagonal rings were added onto the surfaces of the fundamental cross section in different ways with the same cross section area. As the cross sectional shapes considered in their study are quadrangle, hexagon, and those close to hexagon, they concluded that [110] SiNWs exhibiting different patterns at the cross section do not show significant difference in the band gaps. This is verified by our band gap results of rect- and hex-SiNWs. However, as the large geometric discrepancy between tri-SiNW and the other two SiNWs, the band gap variance is remarkable. The large band gap in tri-SiNW is consistent with the idea that the sharp corner structure produces large band gap. [25] Moreover, it is obvious that the band gap of tri-SiNW has stronger size dependence than the band gap of rect-SiNW and hex-SiNW do. For instance, in Fig. 3.5a, the band gap of tri-SiNW decreases 0.86 eV when the dimension increases from 2 nm to 6 nm. However, in the same range the band gap of rect-SiNW only decreases 0.73 eV, and that of hex-SiNW decreases 0.72 eV. The transverse shape effect on the fundamental band gap decreases as the wire dimension is increased and is expected to disappear for very large wires when the band gap approaches that of the bulk material.

The significant cross sectional shape effects on band gap and size dependence can be

understood from the concept of SVR. Due to quantum confinement effect, the band gap increases as the material dimension is reduced, thus leads to an increase of SVR. In other words, SVR has the impact of enlarging band gap. At the same transverse dimension, tri-SiNW has larger SVR than those of the rect-SiNW and hex-SiNW. As a result, its larger SVR induces the largest band gap among those of the rect- and hex-SiNWs, and the strongest size dependence. Our results show how the interaction of the SVR with the quantum confinement effect.

We have used the concept of SVR to explain qualitatively the dependence of band gap on dimension and cross sectional shapes. In the following, we investigate the dependence of band gap on SVR quantitatively. The band gaps versus SVR of the SiNWs are shown in Fig. 3.5b. It is interesting to find that the band gaps of these three SiNWs follow a general relation with SVR. In other words, consistent SVR dependence of band gap is found for SiNWs with any cross sectional shape. The SVR effect on band gap can be described by a universal expression as

$$E_G = E_0 + aS ,$$

where E_0 corresponds to the band gap of bulk silicon, a is an adjustable parameter and S is the value of SVR in unit of nm^{-1}. From our calculated band gaps, the best fitting gives rise to a = 0.37±0.01 eV-nm and E_0 = 1.28±0.02 eV. E_0 here is best fit value of band gap of bulk silicon, which is very close to the direct DFTB calculated band gap (1.29 eV) of bulk silicon.

This universal band gap expression is applicable to [110] SiNWs with any cross sectional shape and area. It is the first formula which relates quantitatively the band gap to SVR of SiNWs. The band gap of SiNWs are usually difficult to measure, but their transverse cross sectional shape and dimension are easy to know, so it is of significance to predict the band gap values of SiNWs by using the above expression. It is noted that the linear SVR relation with band gap does not depend on the specific calculation methods. In Fig. 3.5b, we also show the band gap versus SVR relation based on the results from ref. 15 for hex-SiNWs, calculated with DFT BPW91 functionals, and with the Los Alamos effective-core-potential plus double zeta valence basis set for Si atoms and 6-31G* for H atoms. [15] A good linear SVR dependence also appears from their results (in ref. 15, they showed the band gap vs diameter relation). However, the fitting value for a is 0.24±0.01 eV-nm and E_0 is 1.11±0.05 eV. The results are smaller than those presented in this chapter. The origin of this discrepancy is due to different computational methods are used, and it is well known that there are large differences between band gaps calculated with different DFT functionals. [32] Although the values of the best-fitting parameters are not consistent, the linear SVR dependence of band gap is obvious. This shows the impact of SVR on band gap is an intrinsical phenomenon in nano materials.

The linear SVR dependence of band gap reveals the importance of surface in study of electronic structure of nano materials. It was found that in small SiNWs, the electron band edges have wave function amplitude concentrated in the exterior of the wire. In contrast

to that in bulk material, the true electron wave functions are hollow in the wire centre in SiNW. [33] Therefore, the transverse dimension is not a good "gauge" to describe the electron band gap, and SVR is a better one as it relates directly to the exterior surface. And the obtained linear SVR dependence of the band gap is of practical importance as it allows us to avoid the using of nanowire diameter to discuss the quantum confinement effect on band gap. It must be stressed that the definition of the nanowire's transverse dimension is ambiguous. Indeed in the literatures different transverse dimensions are reported for wires with the same number of atoms in the super cell. [34] This is due to the fact that different definitions of the wire's transverse dimension exist and the irregular cross sectional shape of most wires. The difference between these definitions becomes crucial if we consider small SiNW in the transverse dimension in range of 1–10 nm. In contrast to the ambiguity in the definition of the SiNW transverse dimension, the SVR clearly describes the electron band gap of SiNW. It has the advantage to estimate band gap for SiNWs with any cross sectional shapes.

In the study of SiNWs, the cylindrical shape approximation is commonly used. It is well known that the band gap of SiNW increases as the diameter is decreased: $E_G=E_0+C/d^n$, where d is the cylinder diameter [16], n is found to be between 1 and 2. A value of 2 for n is expected by using a cylindrical confinement potential and in an effective-mass particle-in-a-box approach [33], with the infinite barrier height. However, in SiNWs with transverse dimension less than 10 nm, the electron effective mass is not a

constant, which makes the effective mass approximation invalid. [35, 36] More detailed analysis of the quantum confinement effect in the framework of first principles and semi-empirical methods shows that a smaller parameter *n* between 1 and 1.4 are obtained. [16, 34, 36-38] However, the diameters of the wires considered in these studies were too small (less than 3.4 nm) to study the size effects on band gap in a large size range. And the few data (typically less than 5 band gap values) obtained from first principles calculations also limits the accuracy of the fitting equation. In this work, based on a set of data with 22 band gap values, a highly linear dependence of band gap on SVR for SiNWs with transverse dimension up to 7 nm is obtained. This highly linear dependence benefits to the determination of *n* value accurately. In a SiNW with cylindrical shape, the SVR is *~1/d*. As such, the highly linear SVR behavior of the band gap observed for the SiNWs implies an inverse dependence $E_G \sim 1/d$ on the SiNW diameter, determines the value of *n* is equal to 1. This is very close to the value of 1.1 predicted by DFT-LDA calculations corrected with GW approximation. [34]

3.5 Conclusions

In conclusion, with DFTB calculations, we have systematically studied the electronic structures of [110] oriented SiNWs. [110] SiNWs remain direct band gap with transverse dimension up to 7 nm. The band gap of SiNW increases as the transverse dimension is

decreased. With the same transverse dimension, the tri-SiNW has the largest band gap among those of rect- and hex-SiNWs. Most interestingly, a linear dependence of band gap on SVR is found for the first time, which is independent of the specific cross sectional shape. In other words, a universal band gap expression is demonstrated for [110] SiNWs with any cross sectional shapes. The using of SVR is of practical importance as it allows us to avoid the ambiguous definition of the nanowire's diameter. Intrinsically, the linear SVR dependence is related to the inverse relation between the band gap and the transverse dimension in small SiNWs. Our results show that in addition to the important factor for the reactivity in chemical reactions, SVR is also a key role on electronic band structure of nano materials.

Acknowledgement

The work is supported by grant R-144-000-203-112 from Ministry of Education of Republic of Singapore and grant R-144-000-222-646 from NUS.

References

[1] Cui, Y.; Wei, Q. Q.; Park, H. K.; Lieber, C. M. *Science* **2001,** *293*, 1289.

[2] Cui, Y.; Lieber, C. M. *Science* **2001,** *291*, 851.

[3] Vo, T. T.M.; Williamson A. J.; Lordi V.; Galli G. *Nano Letters* **2008**, *8*, 1111.

[4] Hochbaum, A. I.; Chen, R.; Delgado, R. D.; Liang, W.; Garnett, E. C.; Najarian, M.; Majumdar, A.; and Yang, P. D. Nature, **2008**, *451*, 163.

[5] Boukai, A. I.; Bunimovich, Y.; Tahir-Kheli, J.; Yu, J.-K.; Goddard III, W. A.; and Heath, J. R. Nature, **2008**, *451*, 168.

[6] Yang, N.; Zhang, G.; and Li, B. W. Nano Letters, **2008**, *8*, 276.

[7] Tian, B.; Zheng, X.; Kempa, T. J.; Fang, Y.; Yu, N.; Yu, G.; Huang, J.; Liber, C. M. Nature, **2007**, *449*, 885.

[8] Duan, X. F.; Huang, Y.; Cui, Y.; Wang, J. F.; Lieber, C. M. *Nature* **2001,** *409*, 66.

[9] Ma, D. D. D.; Lee, C. S.; Au, F. C. K.; Tong, S. Y.; Lee, S. T. *Science* **2003,** *299*, 1874.

[10] Zhang, R. Q.; Lifshitz, Y.; Lee, S. T. *Advanced Materials* **2003,** *15*, 635.

[11] Friedman, R. S.; McAlpine, M. C.; Ricketts, D. S.; Ham, D.; Lieber, C. M. *Nature* **2005,** *434*, 1085.

[12] Sirbuly, D. J.; Law, M.; Yan, H. Q.; Yang, P. D. *Journal of Physical Chemistry B* **2005,** *109*, 15190.

[13] Fernandez-Serra, M.-V.; Hadéis, Ch.; and Blase, X. Nano Letters, **2006**, *6*, 2674.

[14] Rurali, R.; and Lorente, N. Phys. Rev. Lett., **2005**, *94*, 026805.

[15] Ng, M.-F.; Zhou, L.; Yang, S.-W.; Sim, L. Y.; Tan, V. B. C.; and Wu, P. Phys. Rev. B, **2007**, *76*, 155435.

[16] Yan, J. A.; Yang, L.; Chou, M. Y. *Physical Review B* **2007,** *76*, 115319.

[17] Vo, T.; Williamson, A. J.; Galli, G. *Physical Review B* **2006,** *74*, 045116.

[18] Nolan, M.; O'Callaghan, S.; Fagas, G.; and Greer, J. C. *Nano Letters* **2007**, 7, 34.

[19] Kudrawiec, R.; Nyk, M.; Syperek, M.; Podhorodecki, A.; Misiewicz, J.; Strek, W. *Applied Physics Letters* **2006,** *88*, 3.

[20] Jie, J. S.; Zhang, W. J.; Jiang, Y.; Meng, X. M.; Li, Y. Q.; Lee, S. T. *Nano Letters* **2006,** *6*, 1887.

[21] Zhang, R. Q.; Lifshitz, Y.; Ma, D. D. D.; Zhao, Y. L.; Frauenheim, T.; Lee, S. T.; Tong, S. Y. *Journal of Chemical Physics* **2005,** *123*, 144703.

[22] Wang, J.; Rahman, A.; Klimeck, G.; Lundstrom, M. *IEEE International Electron Devices Meeting (IEDM) Tech. Digest*, Dec. 5-7, Washington D. C., **2005**, 537.

[23] Pennelli, G.; Piotto, M. *Journal of Applied Physics* **2006,** *100*, 054507.

[24] De Vlaminck, I.; De Greve, K.; Lagae, L.; Borghs, G. *Applied Physics Letters* **2006,** *88*, 063112.

[25] Cao, J. X.; Gong, X. G.; Zhong, J. X.; Wu, R. Q. *Physical Review Letters* **2006,** *97*, 136105.

[26] Leao, C. R.; Fazzio, A.; da Silva, A. J. R. *Nano Letters* **2007,** *7*, 1172.

[27] Wu, Y.; Cui, Y.; Huynh, L.; Barrelet, C. J.; Bell, D. C.; Lieber, C. M.

Nano Letters **2004,** *4*, 433.

[28] Elstner, M.; Porezag, D.; Jungnickel, G.; Elsner, J.; Haugk, M.; Frauenheim, T.; Suhai, S.; Seifert, G. *Physical Review B* **1998,** *58*, 7260.

[29] Frauenheim, T.; Seifert, G.; Elstner, M.; Hajnal, Z.; Jungnickel, G.; Porezag, D.; Suhai, S.; Scholz, R. *Physica Status Solidi B-Basic Research* **2000,** *217*, 41.

[30] Zheng, G. S.; Irle, S.; Morokuma, K. *Chemical Physics Letters* **2005,** *412*, 210.

[31] Ashcroft, N. W.; and Mermin, N. D. Solid State Physics (Saunders College, Philadelphia, PA, 1976).

[32] Zhang, G.; and Musgrave, C. B. J. Phys. Chem. A, **2007**, *111*, 1554.

[33] Yeh, C.-Y.; Zhang, S. B.; and Zunger, A. Phys. Rev. B, **1994**, *50*, 14405.

[34] Bruno, M.; Palummo, M.; Ossicini, S.; and Del Sole, R. Surface Science, **2007**, *601*, 2707.

[35] Niquet, Y. M.; Lherbier, A.; Quang, N. H.; Fernandez-Serra, M. V.; Blase, X.; and Delerue, C. Phys. Rev. B, **2006**, *73*, 165319.

[36] Delerue, C.; Allan, G.; and Lannoo, M. Phys. Rev. B, **1993**, *48*, 11024.

[37] Leu, P. W.; Shan, B.; and Cho, Kj. Phys. Rev. B, **2006**, *73*, 195320.

[38] Delley, B; Steigmeier, E. F. *Applied Physics Letters* **1995,** *67*, 2370.

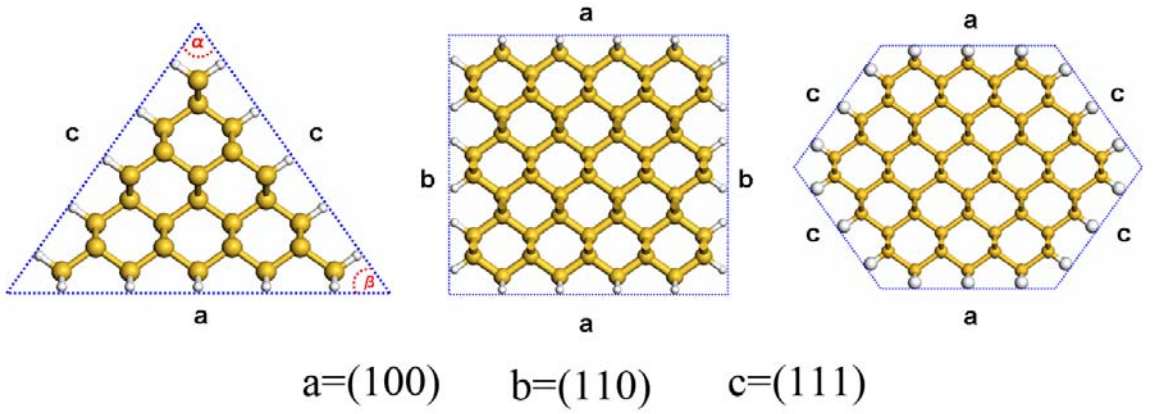

Figure 3.1: (Color online) Schematic diagrams of the SiNWs used in our calculations. From left to right, they are the tri-, rect- and hex-SiNWs. In tri-SiNW, the angle α is 70.6º and β is 54.7º, where this structure is in accordance with the nanowires studied in the experimental work in Ref. 23. The blue dotted lines represent the virtual cages used to construct the SiNWs. Si and H atoms are represented in yellow and white, respectively.

Table 3.1: Transverse dimension D (in nm), cross section area A (in nm^2) and the number of atoms N in the supercell in our calculations. The dimension D is defined as the largest distance between the terminating hydrogen atoms in the cross section plane.

Tri-SiNW			Rect-SiNW			Hex-SiNW		
N	D (nm)	A(nm^2)	N	D(nm)	A(nm^2)	N	D (nm)	A(nm^2)
90	1.79	0.83	96	1.66	1.09	80	1.40	1.05
154	2.56	1.88	164	2.28	2.29	156	2.17	2.50
234	3.32	3.34	288	3.22	4.69	256	2.94	4.58
330	4.09	5.21	396	3.85	6.93	380	3.71	7.29
442	4.86	7.51	520	4.50	9.59	528	4.48	10.63
570	5.63	10.22	724	5.43	14.08	700	5.24	14.58
714	6.40	13.35	888	6.08	17.78	896	6.01	19.17
874	7.16	16.89						

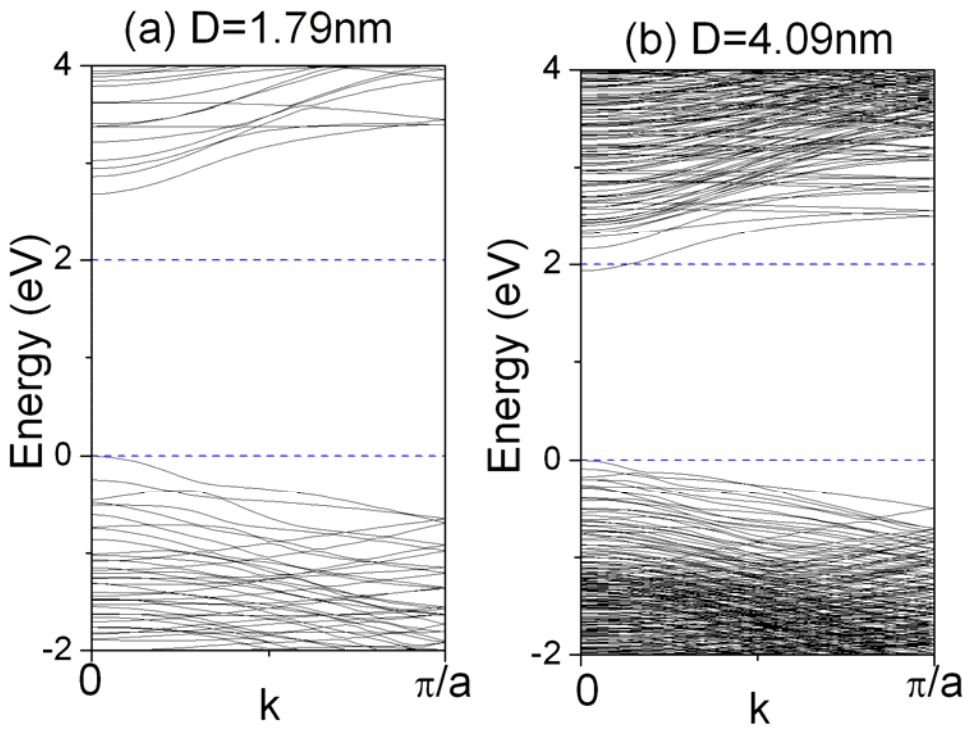

Figure 3.2: Energy band structure for tri-SiNWs with transverse dimension of (a) D=1.79 nm and (b) D=4.09 nm. The valence band maximum has been shifted to zero. The blue dotted lines are drawn to guide the eyes.

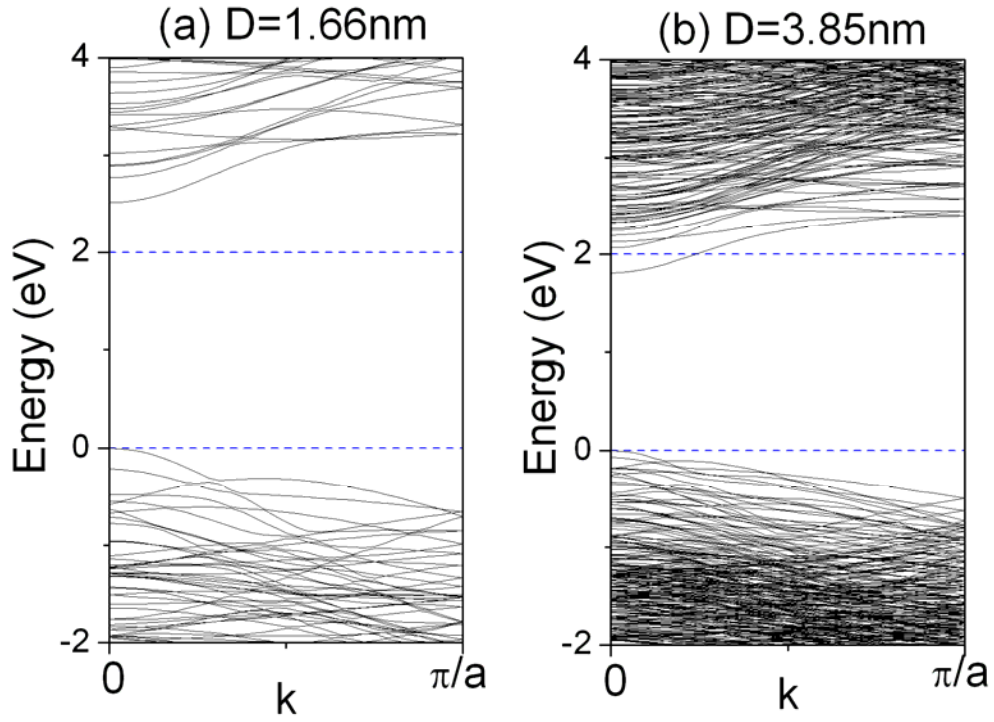

Figure 3.3: Energy band structure for rect-SiNWs with transverse dimension of (a) D=1.66 nm and (b) D=3.85 nm. The valence band maximum has been shifted to zero. The blue dotted lines are drawn to guide the eyes.

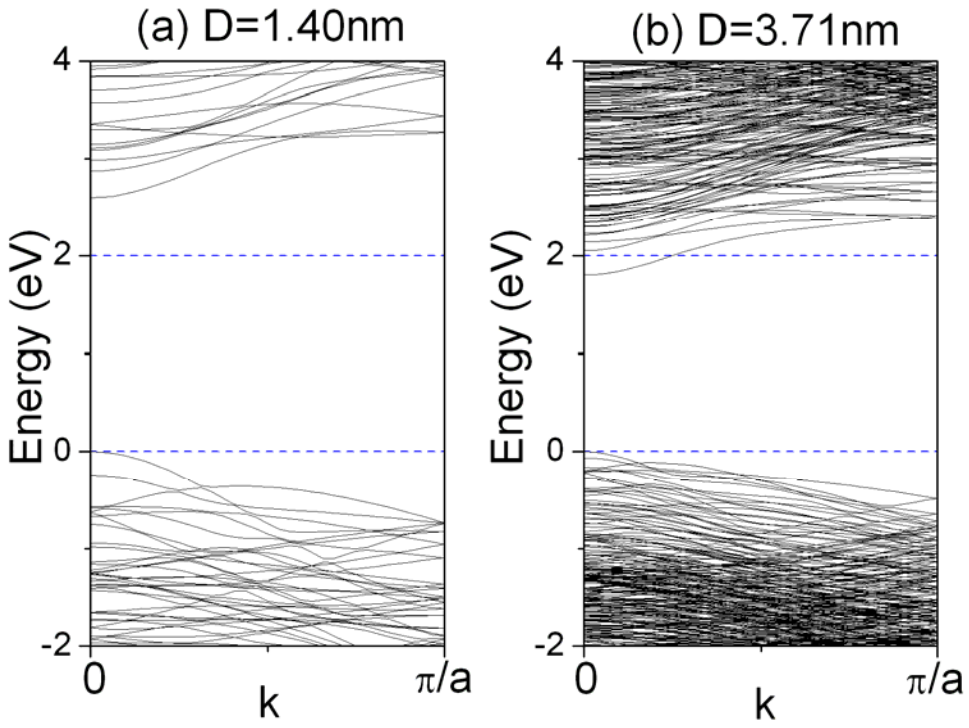

Figure 3.4: Energy band structure for hex-SiNWs with transverse dimension of (a) D=1.40 nm and (b) D=3.71 nm. The valence band maximum has been shifted to zero. The blue dotted lines are drawn to guide the eyes.

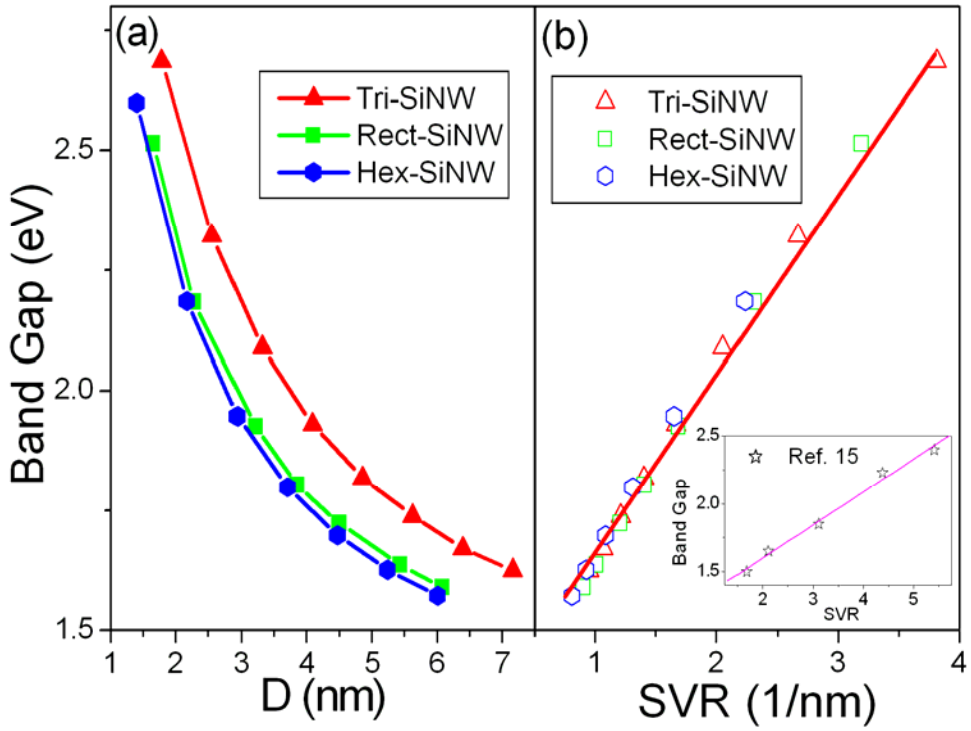

Figure 3.5: (a) Band gap versus the transverse dimension D. (b) Band gap versus SVR. The red solid line is the best-fit one with slope 0.37±0.01 eV-nm. Inset of (b) is the band gap versus SVR relation based on the results from Ref. 15 for hex-SiNWs.

Chapter 4

Impacts of Size and Cross-Sectional Shape on Surface Lattice Constant and Electron Effective Mass of Silicon Nanowires

We investigate the surface lattice and electronic structure of [110] oriented hydrogen-passivated silicon nanowires (SiNWs) of different cross sectional shapes by using the first-principles tight binding method. Remarkable quantum confinement effects are observed on the surface lattice constant and the electron effective mass. Moreover, with the same cross sectional area, the triangular-SiNW has more obvious size dependence than rectangular-SiNW. The significant size and cross-sectional shape effects are explained by the concept of surface-to-volume ratio. Our results demonstrate that due to the smaller electron effective mass, the rectangular-SiNW has obvious advantage over triangular-SiNW in application in higher ON-current in SiNW transistor

4.1 Introduction

The physical and chemical properties of nano scale materials can be significantly improved as the size is reduced to the nanometer regime. Among these nanoscale materials, one-dimensional systems, such as nanowires and nanotubes are of outstanding current interest as one of the promising building blocks for future nanoscale electronic, optoelectronic, and phononic devices. As the demands of more compact devices emerge, silicon nanowires (SiNWs) have attracted extensive attention due to their compatibility with Si-based electronic technology. The fascinating potential applications [1] such as novel power device [2], thermoelectric materials [3-6] and, biological and mechanical sensors [7, 8] have attracted wide research interests in recently years.

Inspired by experimental works, more and more theoretical efforts have been made to understand the electronic properties of SiNWs. The impacts of the diameter, surfaces reconstruction, and doping have been reported. [3-9] Further developments of SiNW device design require theoretical tools that can provide reasonable quantitative predictions for realistic structures both accurately and time saving. This is hard to achieve with *ab initio* calculations

which can only be applied to systems of limited size. One possible way of improving this situation is to use semi-empirical approach such as single band effective mass approximation, which can handle much larger systems.

It is well known that the ultimate speed of integrated circuits depends on the carrier mobility, which is inversely proportional to the effective mass. So the concept of effective mass plays a key role in nanoscale electronics and photonics device design. It has been found that the effective mass of SiNW increases as the transverse dimension decreases, [10] and the effective mass can also be modified by uniaxial strain. [11] Applying strain is a useful method to modulate band structures and enhance the device performance. It is also a very economical way and has the advantage of being compatible with current CMOS process. The strain can be experimentally realized through depositing a capping layer around the SiNW. At the interface between NW core and the cover layer, the lattice constant mismatch couples to the electronic as well as the optical properties of such system. So it is indispensable to accurately evaluate surface lattice constant of SiNWs. Although some researches have been done, many important and fundamental questions remain unsolved. For example, what is the quantum confinement

effect on surface lattice constant? And how does the surface lattice constant and electron effective mass depend on nanowire cross-sectional shape?

In this chapter, we present the detailed investigation on the surface lattice constant and electron effective mass of [110] oriented and hydrogen passivated SiNWs with rectangular and triangular cross section shape. These SiNWs can be fabricated experimentally. [12, 13] For simplicity in this chapter, they are named as tri-SiNWs and rect-SiNWs, respectively. We focus on SiNWs oriented along the [110] direction because small diameter SiNWs have been observed to grow experimentally mostly along this direction, and it has been demonstrated that [110] is the optimum orientation that offers the highest ON-current and smallest intrinsic device delay for the same OFF-current for SiNW transistors. [14] In additionl, as there is large effect of acoustic phonon on hole effective mass [15], here we only calculate the electron effective mass from band structure.

4.2 Methodology

Figure 4.1 shows the schematic pictures of the rect- and tri-SiNWs. In the tri-SiNW, α=74 º and β=53 º, where this structure is in accordance with the nanowires studied in the experimental work in Ref. 12. For [110] tri-SiNW, it has two <111> faces and one <100> face. And the rect-SiNW has two <100> faces and two <110> faces. The cross-sectional areas of the SiNWs are ranging from 1 nm^2 to about 18 nm^2. For each NW, the atomic structure is initially constructed by selecting all the Si atoms that fall within a virtual cage placed in diamond structured bulk silicon while silicon atoms falling outside this virtual cage are removed. The surface dangling bonds are terminated with hydrogen atoms with a standard bond length of 1.48 Å that eliminate artificial dangling bonds. This Si-H bond length corresponds to that in SiH_4 molecule. Although surface reconstruction may have effects on the band structure of SiNWs, here we exclude such factor and concentrate on the size and transverse cross sectional shape effects of SiNWs. Therefore, no surface reconstruction is considered in this study. This H-termination model without surface reconstruction is widely used to study the size effect on electronic structure of SiNWs. [16, 17] A supercell approach is adopted where the SiNW is periodically repeated along the growth direction. The length of the supercell along the longitudinal direction is determined from the calculated lattice

constant of bulk silicon to keep the wire is unstrained. The size of the supercells in the transverse plane is larger than 15 Å so as to avoid the cell to cell interaction. The atoms are free to move in all three directions because the radius of the unit cell is larger than the radius of the nanowire.

The calculations are carried out with the density functional derived tight-binding method (DFTB). [18-20] The DFTB scheme is in a self-consistent charge (SCC) mode. The energy minimization scheme is the conjugate gradient method. A 32×1×1 Monkhorst-Pack k-point sampling is used for integration of the first Brillouin zone. The optimization is performed until the forces on the atoms are less than $3x10^{-4}$ au and the tolerance in the self-consistent charge is 10^{-5} au. Good convergence is obtained with these parameters. This DFTB scheme has been verified an optimal compromise of accuracy, system size, and computation time compared to pure first-principles methods. The DFTB scheme allows the simulation of larger systems than the conventional DFT at a reasonable computational time with similar accuracy. In assessing the accuracy of the computational method, we have performed calculations for the lattice constant of bulk silicon. The calculated value, 5.46

Å, is close to the experimental values (5.43 Å), providing support for the accuracy of the current model.

4.3 Results and discussion

The initial geometries are relaxed to their closest minimum total energy. Then, the surface lattice constant is calculated from the average Si-Si atom distances on the surface. The dependence of surface lattice constant on SiNW transverse dimension is shown in figure 4.2. Here a_0 is the calculated lattice constant of bulk silicon, 5.46 Å. It is obvious that the surface lattice constants of SiNWs are smaller than that of bulk silicon. This is in consistent with the results calculated with first-principles generalized gradient approximation (GGA) method. [21] It is found that the surface lattice constants of the SiNWs increases with the transverse dimensions of the wires increase. This shows that the quantum confinement effect on surface lattice constant remains in a large transverse dimension range. The dependence of surface lattice constant on dimension is consistent with the experimental observation for semiconductor nanoparticles. [22] When the transverse cross sectional area increases from 1 nm^2 to about 18 nm^2, the surface lattice constant increases about 1%. It is

worth pointing that this 1% lattice mismatch will induce observable effect on the band structure. It has been demonstrated that 1-2% lattice mismatch can lead to obvious modulation on band structure and band gap of SiNWs. [11, 21] For instance, a +1% strain can decrease the band gap of 0.1 eV [11]. Experimentally, the lattice strain can be realized through epitaxial growth of SiGe or Ge on top of a SiNW. Because the lattice constant of Ge (SiGe) is greater than that of Si (by <4%), and as the surface lattice constant of small SiNW is smaller than that of large SiNW, SiNW of small diameter has larger strain than SiNW of larger diameter does, and corresponds to larger modulation on band gap. In addition to the size dependence, the surface lattice constants of the tri-SiNWs are smaller than those of the rect-SiNWs with the same cross sectional area, and the differences between the two kinds of wires decrease as the increase of the diameter. The significant size and transverse cross-sectional shape effects on the surface lattice constant can be understood from the increase of surface energy in nanoscale materials. Nano materials have a high surface area to volume ratio (SVR) and correspond to high surface energy. To lower the total energy, surface atoms will shrink and reduce the surface lattice constant. In other words, SVR has the impact of reducing the surface lattice constant. So the surface lattice constant of SiNW is smaller than

that of bulk silicon, and increases with the transverse dimension increases (corresponds to reduce SVR). At the same transverse dimension, tri-SiNW has larger SVR than that of the rect-SiNW. As a result, it has smaller surface lattice constant than that of rect-SiNW.

After the optimized structures for these SiNWs are obtained, we figure out the band structures and electron effective mass (m*) at conduction band minimum (CBM). Figure 4.3 shows the calculated band structure for [110] oriented SiNWs. Here we only show the lowest CBM structures of tri-SiNW and rect-SiNW. As well known, bulk silicon has an indirect band gap. With the dimensions of silicon are reduced from the bulk to nano scale, quantum confinement effect increases the band gap of the system. For nanostructured wires with sufficiently small dimensions, a transition from an indirect to direct gap material occurs. The band structures shown in Fig 4.3(a) and 4.3(b) are generally consistent to those calculated by first principles methods. [9] It is worth pointing out that in order to justify the characteristic of band gap (direct band) more accurately, systematic calculations on the dipole transition matrix elements for optical adsorption are necessary. [23] The dependence of CBM on SiNW transverse dimensions are shown in Fig. 4.3(c) and 4.3(d). As the

magnitude of the energy increases at Γ point is faster than those close to Γ point, the curvature of the lowest CBM of SiNW is smaller than that of bulk silicon and induces larger effective mass. More interesting, the curvature of the lowest CBM decreases with the transverse dimension decreases, and corresponds to large effective mass.

As the parabolic approximation of the energy dispersion is still accurate at the lowest CBM of SiNW [24], in the following, we investigate the dependence of electron effective mass on dimension and transverse cross-sectional shape quantitatively. The dependence of electron effective mass on SiNW transverse cross-sectional area is shown in Fig. 4.4. It is obvious that the smaller the dimension of the wire the larger the electron effective mass due to quantum confinement. For thick wires, the effective mass of electron is close to that of bulk Si (0.2 m_e, m_e is the free electron mass), which is consistent with other reports. [14] However, the values of effective mass presented in this letter are smaller than those in Ref. 14. The origin of this discrepancy is due to different computational methods are used, and it is well known that there are large differences between electronic structure calculated with different DFT functionals. [25] Although the values of effective mass are not consistent, the

size effect is obvious. In addition to the size dependence, the most interesting feature we should like to point out is that the electron effective mass also shows significantly different change with respect to the cross-sectional shape. The electron effective masses of the tri-SiNWs are always larger than those of the rect-SiNWs with the same cross-sectional area, and the transverse shape effect on the electron effective mass decreases as the wire dimension is increased and is expected to disappear for very large wires. Moreover, it is obvious that the effective mass of tri-SiNW has stronger size dependence than the effective mass of rect-SiNW does. For instance, in Fig. 4.4, the effective mass in tri-SiNW decreases 0.04 m_e when the cross sectional area increases from 1 nm^2 to 18 nm^2. However, in the same range the electron effective mass of rect-SiNW only decreases 0.02 m_e. The significant cross sectional shape effects on effective mass and size dependence are also contributed from the concept of SVR. As we discussed above, due to quantum confinement effect, the electron effective mass increases as the material dimension is reduced, thus leads to an increase of SVR. So SVR has the impact of increasing the effective mass. The SVR dependence of effective mass reveals the importance of surface in study of electronic structure of nano materials. The physical mechanism is that in small SiNWs, the true electron wave functions are

hollow in the wire center in SiNW and concentrated in the exterior of the wire. As a result, with the same transverse dimension, the larger SVR of tri-SiNW leads to the stronger size dependence than rect-SiNW does, and corresponds to larger effective mass. From the discussion in ref. 14, when m* is relatively large (e.g., $m^*>0.15\ m_e$), the device is operating close to the charge control limit, and the ON-current increases with a decreasing m*. Since rect-SiNW has smaller m*, we proposed that it can offer higher ON-current than tri-SiNW in SiNW transistor performance.

4.4 Conclusion

In this chapter, we have studied surface lattice constants, band structure and electron effective mass of the tri-SiNWs and rect-SiNWs with first-principles tight-binding method (other shapes are not including in this chapter). With this method, we can explore the properties of SiNWs with transverse cross sectional area up to 18 nm^2, which is larger than the structures studied with common used DFT methods. It is found that the surface lattice constants of SiNWs increases with the transverse dimension of the wire increases. The electron effective mass decreases with the SiNW transverse dimension (cross

sectional area) increases. With the same cross sectional area, the tri-SiNW has larger electron effective mass than that of rect-SiNW. And in tri-SiNW, the dependence of electron effective mass on cross section area is more obvious than that in rect-SiNW. The quantum confinement effects on surface lattice constant and effective mass, and the impacts of transverse cross sectional shape are well explained by the concept of surface-to-volume ratio. SVR has the impacts of reducing the surface lattice constant and increasing the electron effective mass. At the same transverse dimension, tri-SiNW has larger SVR than that of the rect-SiNW. As a result, it has larger electron effective mass than that of rect-SiNW. Our results demonstrate that rect-SiNW has obvious advantage over tri-SiNW in application for higher ON-current in SiNW.

Acknowledgement.

The work is supported in part by grant R-144-000-203-112 from Ministry of Education of Republic of Singapore and grant R-144-000-222-646 from NUS.

References

[1] Y. Li, F. Qiang, J. Xiang, C. M. Lieber, Materials Today **9**, 18 (2006).

[2] B. Tian, X. Zheng, T. J. Kempa, Y. Fang, N. Yu, G. Yu, J. Huang, C. M. Lieber, Nature **449**, 885 (2007).

[3] T. T. M. Vo, A. J. Williamson, V. Lordi, G. Galli, Nano Lett. **8**, 1111 (2008).

[4] A. I. Hochbaum, R. Chen, R. D. Delgado, W. Liang, E. C. Garnett, M. Najarian, A. Majumdar, P. D. Yang, Nature **451**, 163 (2008).

[5] A. I. Boukai, Y. Bunimovich, J. Tahir-Kheli, J.-K. Yu, W. A. Goddard III, J. R. Heath, Nature **451**, 168 (2008).

[6] N. Yang, G. Zhang, B. W. Li, Nano Lett. **8**, 276 (2008).

[7] Y. Cui, Q. Q. Wei, H. K. Park, C. M. Lieber, Science **293**, 1289 (2001).

[8] Y. Cui, C. M. Lieber, Science **291**, 851 (2001).

[9] T. Vo, A. J. Williamson, G. Galli, Phys. Rev. B **74**, 045116 (2006).

[10] E. Gnani, S. Reggiani, A. Gnudi, P. Parruccini, R. Colle, M. Rudan, G. Baccarani, IEEE Transactions On Electron Devices **54**, 2243 (2007).

[11] D. Shiri, Y. Kong, A. Buin, M. Anantram, Appl. Phys. Lett. **93**, 073114 (2008).

[12] R. Q. Zhang, Y. Lifshitz, S. T. Lee, Adv. Mater. **15**, 635 (2003).

[13] X. F. Duan, Y. Huang, Y. Cui, J. F. Wang, C. M. Lieber, Nature **409**, 66 (2001).

[14] J. Wang, A. Rahman, G. Klimeck, M. Lundstrom, IEEE International Electron Devices Meeting (IEDM) Tech. Digest, pp. 537-540, Washington D. C., Dec. 5-7 (2005).

[15] A. K. Buin, A. Verma, A. Svizhenko, M. P. Anantram, Nano Lett. **8**, 760 (2006).

[16] M.-F. Ng, L. Zhou, S.-W. Yang, L. Y. Sim, V. B. C. Tan, P. Wu, Phys. Rev. B **76**, 155435 (2007).

[17] J. A. Yan, L. Yang, M. Y. Chou, Phys. Rev. B **76**, 115319 (2007).

[18] M. Elstner, D. Porezag, G. Jungnickel, J. Elsner, M. Haugk, T. Frauenheim, S. Suhai, G. Seifert, Phys. Rev. B **58**, 7260 (1998).

[19] T. Frauenheim, G. Seifert, M. Elstner, Z. Hajnal, G. Jungnickel, D. Porezag, S. Suhai, R. Scholz, Phys. Status Solidi B **217**, 41 (2000).

[20] T. Frauenheim, G. Seifert, M. Elstner, T. Niehaus, C. Kohler, M. Amkreutz, M. Sternberg, Z. Hajnal, A. Di Carlo, S. Suhai, J. Phys.: Condens. Matter **14**, 3015 (2002).

[21] K. Hong, J. Kim, S. Lee, J. Shin, Nano Lett. **8**, 1335 (2008).

[22] A. N. Goldstein, C. M. Echer, A. P. Alivisatos, Science **256**, 1425 (1992).

[23] B. Yan, G. Zhou, X. Zeng, J. Wu, B. Gu and W. Duan, Appl. Phys. Lett. **91**, 103107 (2007).

[24] K. Nehari, N. Cavassilas, F. Michelini, M. Bescond, J. L. Autran, M. Lannoo, Appl. Phys. Lett. **90**, 132112 (2007).

[25] G. Zhang, C. B. Musgrave, J. Phys. Chem. A **111**, 1554 (2007).

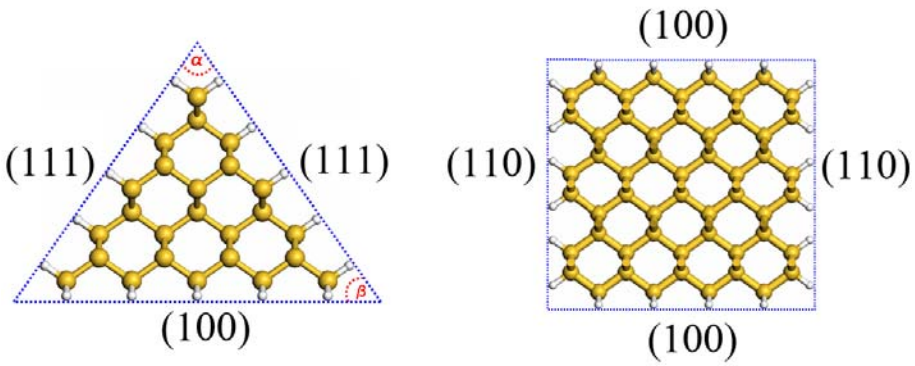

Figure 4.1: Schematic diagrams of the tri-SiNW and rect-SiNW used in our calculations. The blue dotted lines represent the virtual cages used to construct the SiNWs. Si and H atoms are represented in yellow and grey, respectively.

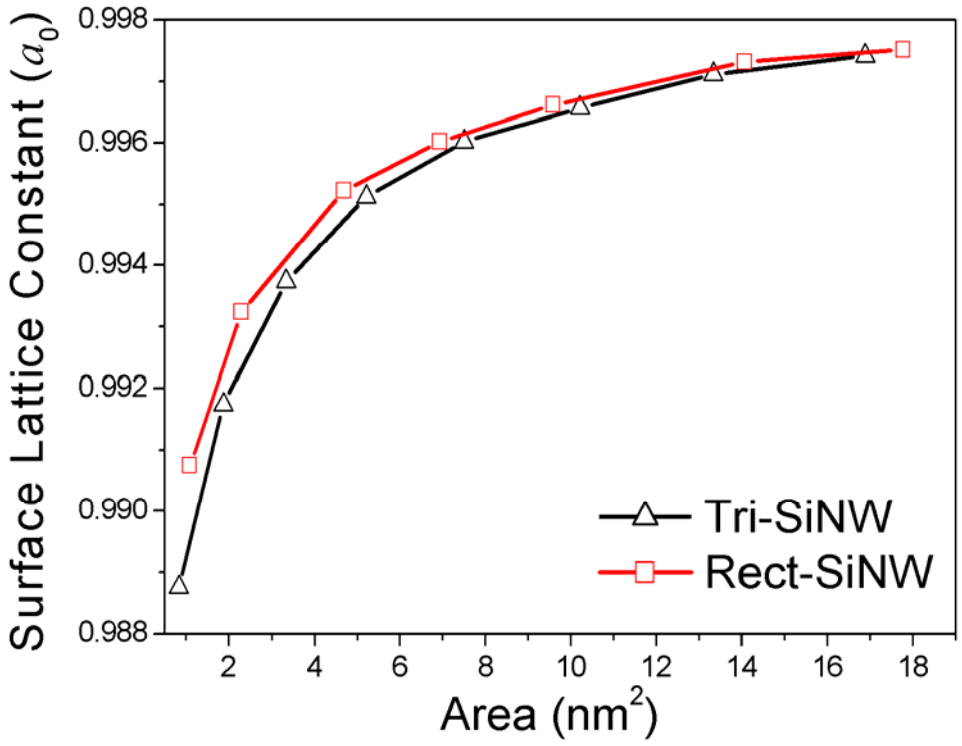

Figure 4.2: The surface lattice constant versus the transverse dimension of SiNWs. a_0=5.46 Å is the calculated lattice constant of bulk silicon.

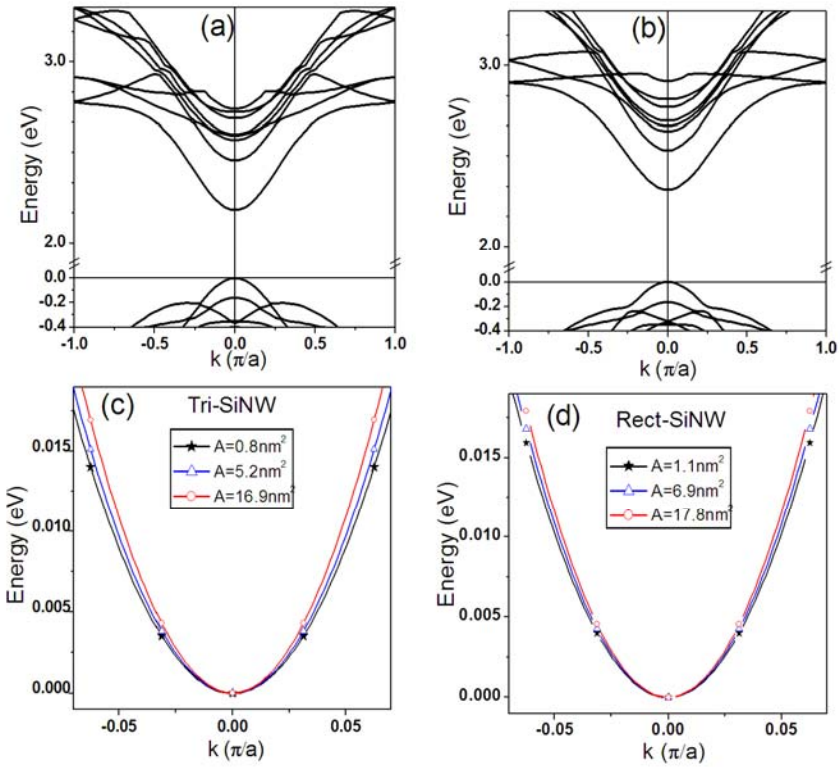

Figure 4.3: (a) Energy band structure for tri-SiNWs with cross sectional area A=1.9 nm^2. (b) Energy band structure for rect-SiNWs with A=2.3 nm^2. In (a) and (b), the valence band maximum has been shifted to zero. (c) The lowest CBM for tri-SiNWs with different transverse dimensions. (d) The lowest CBM for rect-SiNWs with different transverse dimensions. In (c) and (d), the CBM has been shifted to zero. The symbols are DFTB simulation results, and the solid lines are the best-fit ones with parabolic approximation.

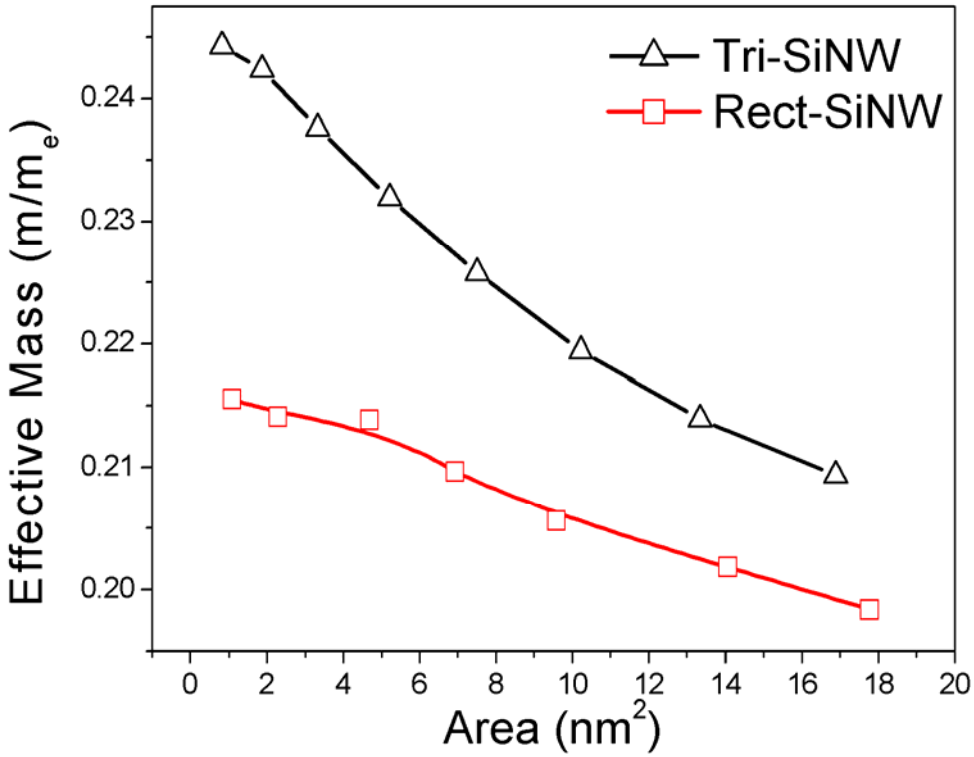

Figure 4.4: The electron effective mass versus the transverse cross sectional area for tri- and rect-SiNWs. m_e is the mass of free electron.

Chapter 5

Direct to Indirect Band Gap Transition in [110] SiNWs

[110] SiNWs have a direct band gap in the ultrathin diameter regime, whereas the energy difference between the indirect and direct fundamental band gaps progressively decreases as the wire size increases, indicating that larger [110] SiNWs could have an indirect band gap. In this Chapter, we investigate the electronic band structure of [110] silicon nanowires (SiNWs), by using first-principles calculation. A series of quantitative direct-indirect band gap transitional diameter for different cross sectional geometries are obtained, which show that the triangular cross sectional SiNWs has the largest transitional diameter.

5.1 Introduction

Silicon nanowires (SiNWs) have attracted much attention due to their promising properties and fascinating potential applications, such as nano electronics device [1, 2], bio-sensor [3, 4], and thermoelectric power materials[5-8]. Recently, SiNWs attract considerable attention for energy harvesting applications, such as solar cell, due to their unique optical and electrical characteristics. The good absorption for solar energy using SiNW arrays has been demonstrated experimentally and theoretically. [9-11] It is well known that bulk silicon has an indirect band gap, with the valence-band-maximum (VBM) locates at the Γ point and the conduction-band-mimimum (CBM) locates approximately 85% from Γ to X. The indirect band gap characteristic limits the application of silicon in optoelectrics. However, it is demonstrated both experimentally [12, 13] and theoretically [14, 15] that ultra-thin (1.3 nm in diameter) hydrogen-terminated [110] and [111] SiNW are direct band gap semiconductors. The fundamental band gap characteristic is key role in many applications, such as light emission and absorption. It is indicated the possibility of fabricating Si-based visible optical devices.

Obviously, there exists indirect to direct band gap transition. Using first-principles calculations, it has been shown that the indirect-to-direct energy gap transition for [111] SiNWs at a diameter of less than 2.2 nm. [14] However, the situation with [110] SiNW is still unknown, which wires seem to be the most promise candidate for the nanowires electronic device and bio-sensor because the band gaps of [110] SiNWs is the smallest among those of the [100], [112] and [111] wires of the same diameter [16]. Moreover, so far there is no systematic report on the indirect-direct band gap transition, and its dependence on the geometry of SiNWs. As the indirect band gap and consequential weak light absorption remain the bottleneck for their application in optoelectronics/solar PV, a detailed understanding of the indirect-to-direct band transition via diameter is of primary importance to the development of new applications for SiNWs. It could be extremely difficult to get this information from experiments. In this Chapter, we studied the direct to indirect band gap transition when the transverse cross section of SiNW is increased, by using first-principle calculations. An extremely linear dependence on the surface-to-volume ratio is found for both the lowest and second-lowest conduction band edge. More interestingly, the shift rate of the second-lowest conduction band edge is faster than that of the lowest

conduction band edge. From the difference in the shift rates, we predict the critical dimension for direct-indirect band gap transition. Moreover, we discussed the cross section shape dependent critical dimensions.

5.2 Methodology: Density Functional Theory and DMol3

The first-principles calculations were carried out using the linear combination of atomic orbital density-functional theory (DFT) methods implemented in the DMol3 package. [17, 18] The generalized gradient approximation (GGA) in the Perdew-Burke-Ernzerhof (PBE) form and an all-electron double numerical basis set augmented with polarized function (DNP basis set) were chosen for the spin-restricted DFT calculations. [19] A supercell approach is adopted where each wire is periodically repeated along the growth direction [110] (see Figure 5.1). The size of the supercells in the transverse plane is large enough (>20 Å from surface to surface). Self-consistent field calculations are done with a convergence criterion of 10^{-6} Hartree on the total energy. All the structures are fully optimized with a convergence criterion of 0.05 eV/Å for the force and 0.005 Å for the displacement. A real-space global cut-off radius was set to be 4.60 Å. The Gaussian smearing of electron density is applied

with the energy range of 0.1 eV. Only the Γ point was considered in the Brilliouin zone for the geometric optimization. For calculation of electronic properties of SiNWs, the Brilliouin zone was sampled by 1×1×50 k-points using the Monkhorst-Pack scheme, which was shown to be sufficient to present the transition of the electronic band structure around the Fermi energy level.

5.3 Results and Discussion

Figure 5.1 shows the schematic representation of the SiNWs used in calculations. NWs with different cross sectional shapes, including triangular-, rectangular- and hexagonal-SiNWs are investigated. For simplicity, they are named as tri-SiNWs, rect-SiNWs and hex-SiNWs, respectively. The transverse size, *D* is defined as the largest distance between the terminating hydrogen atoms in the cross section plane.

After the optimized structures for these SiNWs are obtained, we figure out the band structures for the SiNWs. In inset of Fig. 5.2, the electron band structure of hex-NWs with cross sections area of 7.29 nm^2 is shown. The band

structures are along the growth direction of the wires. Here we only show the band structure of one hex-SiNW, as the band structures of other SiNWs are similar. Our calculations show that these wires exhibit a direct fundamental band gap at Γ due to band folding. The energy difference between the two lowest conduction band edges, the lowest conduction band edge and the second-lowest conduction band edge, is only 0.1 eV. Our calculation is able to correctly describe the energy band feature around the Fermi level, although the calculated band gap value is underestimated compared with experimental measurement due to the conventional DFT calculations suffer from the systematic underestimation of the band gap. [20]

The surface area to volume ratio (SVR) increases as the system scales down. It has important impacts on electronic structure of nano materials. [21, 22] For example, a linear dependence of band gap on SVR has been demonstrated in SiNWs, which is independent of the cross sectional geometry. From Figure 5.2, it is obvious that in addition to the band gap, the band edges also depend on SVR linearly. Here we set energy of valence-band-maximum (VBM) as zero, and its location is at k=0 point in the size-changing process. With SVR decreases (NW transverse dimension increases), both lowest conduction band

edge and the second-lowest conduction band edge decrease, indicates the decreases of band gap with cross section area. More interestingly, the magnitude of the energy band edge decrease induced by quantum confinement is different for each point in the band structure. The decrease rate of the second lowest conduction band edge is faster than that of the lowest conduction band edge. Therefore, for NWs with sufficiently large dimensions, this difference in energy shifts at different points in the Brillouin zone is large enough to move the band edge at the k=0 point above the one at about k=0.3 π/a, then a transition from a direct to indirect gap material occurs.

The same phenomena occur in the case of tri- and rect-SiNWs. For all the SiNWs, the top of the valence band is always located at the k=0 point. If the conduction-band-minimum (CBM) locates at k=0 (or around k=0.3 π/a) point, it behaves as direct (indirect) band gap semiconductor. We quantify the difference between the direct band gap and the indirect band gap by defining a Δ as the energy difference between the energy of the conduction band edges at the k=0 and around k=0.3 π/a points. By so doing, clearly a positive Δ represents a direct band gap while a negative Δ represents an indirect band gap.

Figure 5.3 shows the dependence of Δ on the surface-to-volume ratio (SVR). SVR is an important quantity when the surface atoms possess high fraction of the total atoms such as the nano thin film (2D), nano wire (1D) or nano particle (0D). It represents how deep the system goes into the quantum region. The higher the SVR, the stronger the quantum effect on the materials properties. As shown in Figure 5.3, Δ depends on SVR linearly. With SVR decreases (transverse dimension increases), Δ decreases until to zero, where the direct-to-indirect band gap transition takes place. If the linear dependence on the SVR is extrapolated linearly, then the critical SVR when direct-to-indirect band gap transition takes place, can be obtained. For tri-SiNW, the critical SVR value is 0.546, which corresponds to 14.69 nm in diameter D. The similar calculation can be done for the rect-SiNWs and hex-SiNWs, the corresponding critical SVR and diameters are shown in Table 1. It is obvious from Table 1 that the SiNWs thicker than those critical diameter values will behave as indirect band gap materials, while SiNWs smaller than those values have direct band gaps. Note that the SiNWs of other orientations studied in the previous works all showed a direct-to-indirect transition only at a sufficiently small size. For example, the [111] SiNW

undergoes a change from direct to indirect band gap as wire diameter increases, and the transition takes place at a considerably small diameter of 2 nm.[14] In sharp contrast, our finding suggests that large-diameter, up to 14 nm [110] SiNW is still a direct gap material. This finding is remarkable and shows the important application of [110] SiNWs in optoelectronic and solar cell areas.

5.4 Conclusion

In this Chapter, the transition of band structure from direct to indirect behavior of small diameter hydrogen-terminated [110] SiNWs has been studied. We successfully estimated the critical dimension where this direct-indirect band gap transition takes place by using the gauge of SVR and the DFT calculation results. It is found that tri-SiNW has the largest transition dimension up to 14 nm in diameter. Therefore tri-SiNW has a wider range of high efficient optoelectronic applications.

In this chapter, because we focus on the transition point of the second minimum in the band curve, our calculation are based on the DFT, which is known as more accurate method, while in the chapter 2, we use the DFTB.

Acknowledgment.

The work is supported in part by grant R-144-000-222-646 from National University of Singapore, and by a SERC Grant, A*STAR, Singapore.

References

[1] A. M. Morales, C. M. Lieber, Science **279**, 208 (1998).

[2] Y. Cui, X. F. Duan, J. T. Hu, C. M. Lieber, J. Phys. Chem. B **104**, 5213 (2000).

[3] Y. Cui, Q. Q. Wei, H. K. Park, C. M. Lieber, Science **293**, 1289 (2001).

[4] G.-J. Zhang, G. Zhang, J. H. Chua, R.-E. Chee, E. H. Wong, A. Agarwal, K. D. Buddharaju, N. Singh, Z. Gao, N. Balasubramanian, Nano Lett. **8**, 1066 (2008).

[5] A. I. Hochbaum, R. Chen, R. D. Delgado, W. Liang, E. C. Garnett, M. Najarian, A. Majumdar, P. Yang, Nature **451**, 163 (2008).

[6] A. I. Boukai, Y. Bunimovich, J. T. Kheli, J.–K. Yu, W. A. Goddard III, J. R. Heath, Nature **451**, 168 (2008).

[7] N. Yang, G. Zhang, B. W. Li, Nano Lett. **8**, 276 (2008).

[8] G. Zhang, Q. X. Zhang, C. T. Bui, G. Q. Lo, B. W. Li, Appl. Phys. Lett. **94**, 213108 (2009).

[9] B. M. Kayes, H. A. Atwater, N. S. Lewis, J. Appl. Phys. **97**, 114302, (2005).

[10] L. Hu, G. Chen, Nano Lett. **7**, 3249 (2007).

[11] J. S. Li, H. Y. Yu, S. M. Wong, G. Zhang, X. W. Sun, G. Q. Lo, D. L. Kwong, Appl. Phys. Lett., **95**, 033102 (2009).

[12] Y. Cui, Z. H. Zhong, D. L. Wang, W. U. Wang, C. M. Lieber, Nano Lett. **3**, 149 (2003).

[13] D. D. D. Ma, C. S. Lee, F. C. K. Au, S. Y. Tong, S. T. Lee, Science **299**, 1874 (2003).

[14] X. Y. Zhao, C. M. Wei, L. Yang, M. Y. Chou, Phys. Rev. Lett. **92**, 236805 (2004).

[15] K.-H. Hong, J. Kim, S.-H. Lee, J. K. Shin, Nano Lett. **5**, 1335 (2008).

[16] R. Q. Zhang, Y. Lifshitz, S. T. Lee, Adv. Mater. **15**, 635 (2003).

[17] B. Delley, J. Chem. Phys. **92**, 508 (1990).

[18] B. Delley, J. Chem. Phys. **113**, 7756 (2000).

[19] J. P. Perdew, K. Burke, M Ernzerhof, Phys. Rev. Lett. **77**, 3865 (1996).

[20] G. Zhang, C. B. Musgrave, J. Phys. Chem. A **111**, 1554 (2007).

[21] D. L. Yao, G. Zhang, B. W. Li, Nano Lett. **8**, 4557 (2008).

[22] D. L. Yao, G. Zhang, G. Q. Lo, B. W. Li, Appl. Phys. Lett. **94**, 113113 (2009).

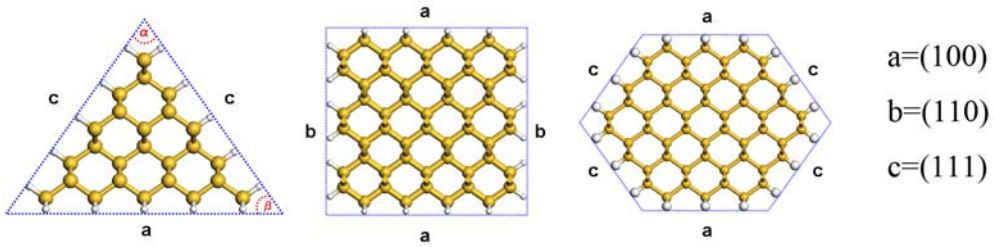

Tri-SiNW Rect-SiNW Hex-SiNW

Figure 5.1: Cross-section view of the 3 types of SiNWs: Tri-SiNW (Triangular cross-section SiNW), Rect-SiNW (Rectangular cross-section SiNW) and Hex-SiNW (Hexagonal cross-section SiNW). a, b and c are the lateral facets, which are (100), (110) and (111), respectively. In Tri-SiNW, the angle α is 70.6º and β is 54.7º. The blue dotted lines represent the virtual cages used to construct the SiNWs. Si and H atoms are represented in yellow and white, respectively.

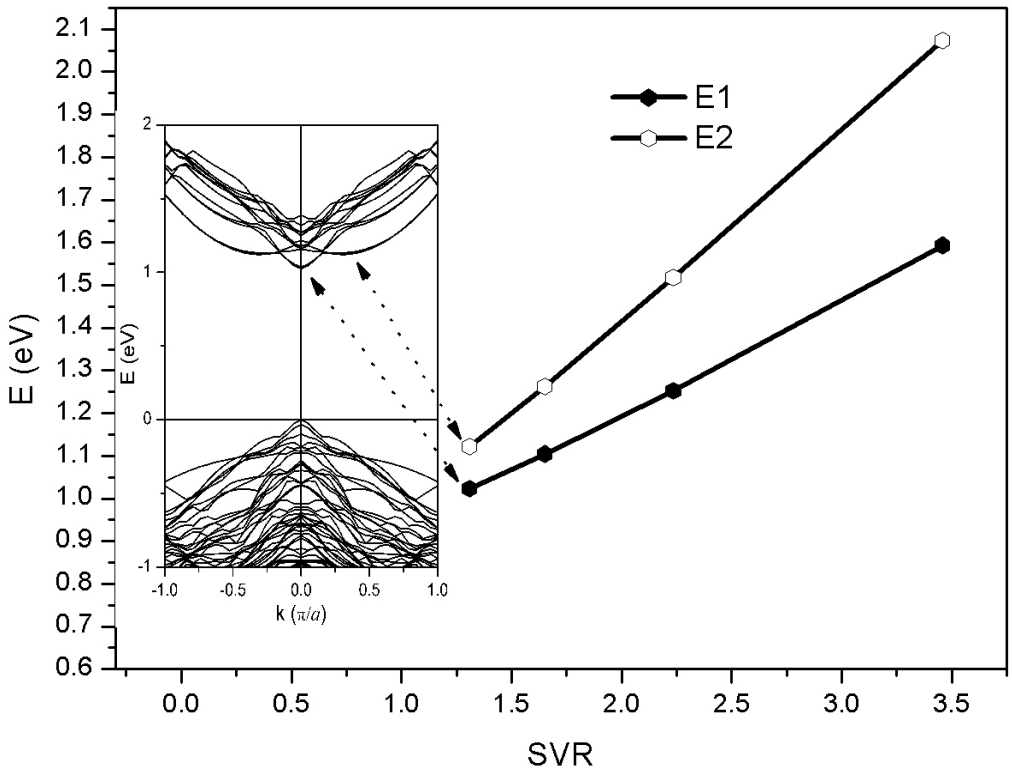

Figure 5.2: The dependence of conduction band edges on the SVR for hex-NWs. Inset is the band structure of hex-NW with cross sections area of 7.29 nm^2.

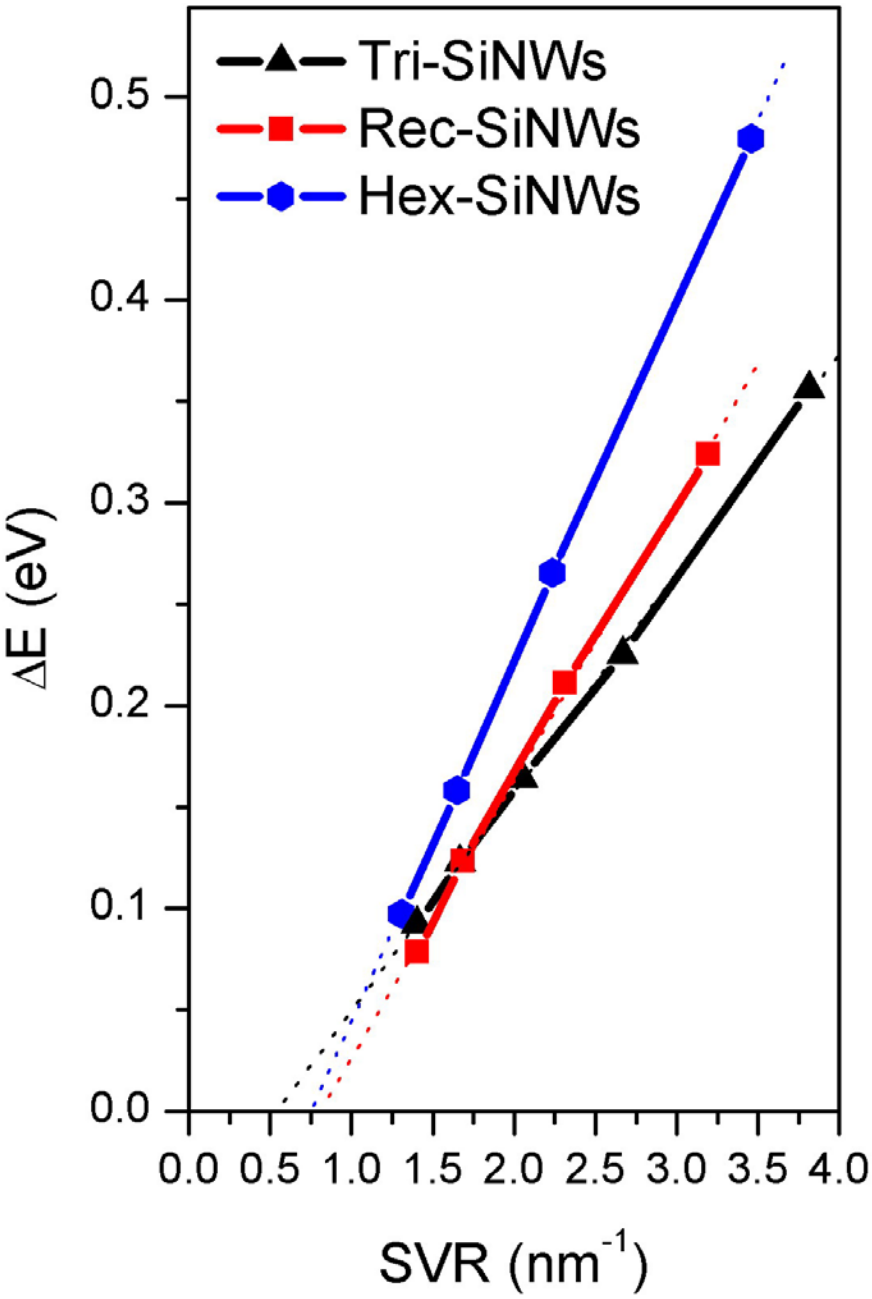

Figure 5.3: (Color online) ΔE versus surface-to-volume ratio (SVR) for tri-, rect-, and hex-SiNWs.

Table 5.1: ΔE versus SVR relationship, critical SVR and diameters for tri-, rect-, and hex-SiNWs studied in this work.

	Tri-SiNW	Rect-SiNW	Hex-SiNW
ΔE (eV)	-0.059+0.108×SVR	-0.108+0.136×SVR	-0.134+0.178×SVR
$SVR\|_{\Delta E=0}(nm^{-1})$	0.546±0.037	0.794±0.064	0.753±0.019
$D\|_{\Delta E=0}(nm)$	14.69±1.00	7.12±0.58	6.84±0.17

Chapter 6

Conclusion and Future Research

6.1 Conclusion

In this thesis, we have been concerned with calculation from first principles, in the framework of density functional theory and density functional based tight binding method, the electronic structure of [110] oriented SiNWs. Detailed studies of the impacts of size, cross sectional shape and surface-to-volume ratio on the electronic band gap, effective mass are carried out.

In Chapter 3, we firstly systematically studied the electronic structure of [110] oriented SiNWs. [110] SiNWs remain direct band gap with transverse dimension up to 7 nm. The band gap of SiNW increases as the transverse dimension is decreased. With the same transverse dimension, the tri-SiNW has the largest band gap among those of rect- and hex-SiNWs. Most interestingly, a linear dependence of band gap on SVR is found for the first time, which is independent of the specific cross sectional shape. In other words, a universal band gap expression:

$$E_G = E_0 + aS$$

where E_0 corresponds to the band gap of bulk silicon, a is an adjustable parameter and S is the value of SVR in unit of nm^{-1}. This expression is demonstrated for [110] SiNWs with any cross sectional shapes. The using of SVR is of practical importance as it allows us to avoid the ambiguous definition of the nanowire's diameter. Intrinsically, the linear SVR dependence is related to the inverse relation between the band gap and the transverse dimension in small SiNWs. Our results show that in addition to the important factor for the reactivity in chemical reactions, SVR is also a key role on electronic band structure of nano materials. It is the first formula which relates quantitatively the band gap to SVR of SiNWs. The band gap of SiNWs are usually difficult to measure, but their transverse cross sectional shape and dimension are easy to know, so it is of significance to predict the band gap values of SiNWs by using the above expression. It is noted that the linear SVR relation with band gap does not depend on the specific calculation methods.

In Chapter 4, we investigated the lattice constant and the electron effective mass of [110] oriented hydrogen-passivated silicon nanowires (SiNWs) of different cross sectional shapes by using the first-principles tight binding method. We explore the properties of SiNWs with transverse cross sectional

area up to 18 nm^2, which is larger than the structures studied with common used DFT methods. It is found that the surface lattice constants of SiNWs increases with the transverse dimension of the wire increases. The electron effective mass decreases with the SiNW transverse dimension (cross sectional area) increases. With the same cross sectional area, the tri-SiNW has larger electron effective mass than that of rect-SiNW. And in tri-SiNW, the dependence of electron effective mass on cross section area is more obvious than that in rect-SiNW. The quantum confinement effects on surface lattice constant and effective mass, and the impacts of transverse cross sectional shape are well explained by the concept of surface-to-volume ratio. SVR has the impacts of reducing the surface lattice constant and increasing the electron effective mass. At the same transverse dimension, tri-SiNW has larger SVR than that of the rect-SiNW. As a result, it has larger electron effective mass than that of rect-SiNW. Our results demonstrate that rect-SiNW has obvious advantage over tri-SiNW in application for higher ON-current in SiNW.

In Chapter 5, we are trying to find the direct to indirect band gap transition in [110] SiNWs. As we know, [110] SiNWs have a direct band gap in the ultrathin diameter regime, whereas the energy difference between the indirect and direct fundamental band gaps progressively decreases as the wire size

increases, indicating that larger [110] SiNWs could have an indirect band gap. We successfully estimated the critical dimension where this direct-indirect band gap transition takes place by using the gauge of SVR and the DFT calculation results. It is found that tri-SiNW has the largest transition dimension up to 14 nm in diameter. Therefore tri-SiNW has a wider range of high efficient optoelectronic applications. The SVR again proved to be an important and useful gauge parameter in the research of material in nano-scale regime.

In a summery, we obtained a universal expression of band gap for silicon nanowires [110] of different cross-section geometries, based on the quantity of SVR (surface-to-volume ratio); we studied the impacts of size and cross-sectional shape on surface lattice constant and electron effective mass of silicon nanowire; we also try to find out the direct to indirect band gap transition dimension in [110] silicon nanowires.

6.2 Future research

In our research group, the main branch is the thermal / heat management, and recent hot topic on the thermal electric materials, so what we did in this thesis

is mainly focused on the electronic part, which is also an important factor to the ZT (figure of merit). The future work will be finding the high ZT materials in 2D or 1D system in the size of nano-scale regime. We are looking into the Si/Ge superlattice/multilayer 2D structures thermal cooler in experiments.

Effective cooling is essential for many high power or low noise electronic and optoelectronic devices. Thermoelectric (TE) refrigeration is a solid-state active cooling method with high reliability. Unlike conventional air-cooling, it can spot cool discrete or localized devices and reduce the temperature of the device below ambient. For a material to be a good thermoelectric cooler, it must have a high value of the dimensionless figure of merit ZT [1] which is given by $ZT=S^2\sigma T/\kappa$, where S is the Seebeck coefficient, σ is the electrical conductivity, T is the temperature, and κ is the thermal conductivity. The use of quantum-well structures to increase ZT was proposed by Hicks and Dresselhaus [2]. Since then much work has been done in the study of superlattice thermoelectric properties, mostly for the in-plane direction [3-6]. The physical origin of the increase in ZT comes mainly from the enhanced density of electron states due to the reduced dimensionality. Recent study shows that superlattice thermal conductivity of cross-plane direction is even lower than that of in-plane direction [7], which can further increase ZT. In

addition, Shakouri and Bowers proposed that heterostructure could be used for thermionic emission to enhance the cooling [8]. Large ZT improvement is possible for the cross-plane transport [9, 10].

SiGe is a good thermoelectric material especially for high temperature applications [11]. Superlattice structures can enhance the cooler performance by reducing the thermal conductivity between the hot and the cold junctions [7, 12], and by selective emission of hot carriers above the barrier layers in the thermionic emission process [8, 9]. In our preliminary work, single element p-type SiGe/Si and Si/Ge superlattice 2D nano structures (Inversed nanowire structure) with electrical transport in the cross-plane direction is demonstrated in figure 6.1 and figure 6.2 below. This paves the road to make n-type and p-type superlattice coolers electrically in series and thermally in parallel, similar to conventional TE coolers, and thus achieve large cooling capacities with relatively small currents.

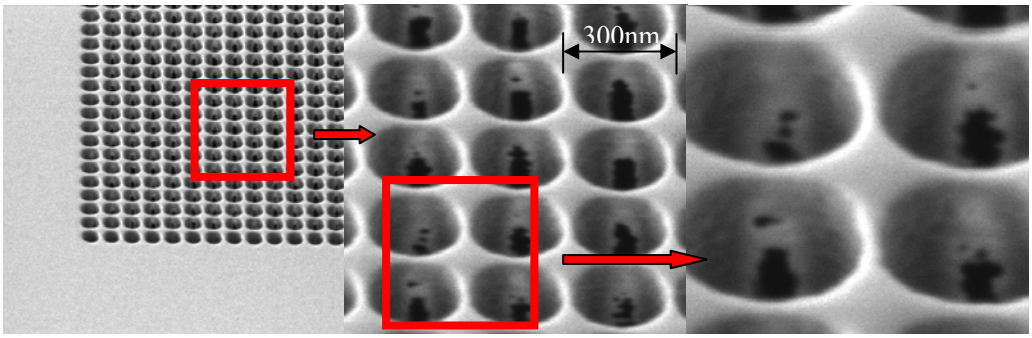

Figure 6.2: Inversed Si/Ge nanowires array (connected).

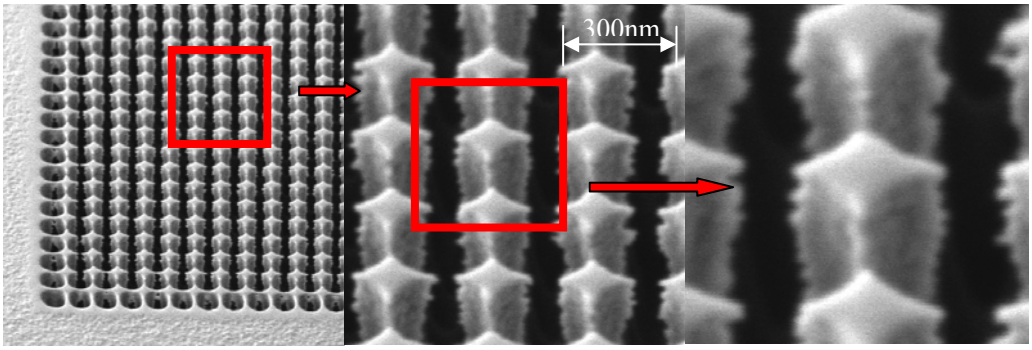

Figure 6.2: Inversed Si/Ge nanowires array (separated).

Reference:

[1]. H. J. Goldsmid, Thermoelectric Refrigeration (Plenum, New York, 1964).

[2]. L. K. Hicks and M.S. Dresselhaus, Phys. Rev. B, 47, 12727 (1993).

[3]. P. J. Lin_Chung and T. L. Reinecke, Phys. Rev. B, 51, 13244 (1995).

[4]. R. Venkatasubramanian, E. Siivola, and T. S. Colpitts, Proceedings of the 17th International Conference on Thermoelectrics, 191 (1998).

[5]. T. Koga, T. C. Harman, S. B. Cornin and M. S. Dresselhaus, Phys. Rev. B, 60, 14286 (1999).

[6]. T. Koga, X. Sun, S. B. Cronin and M. S. Dresselhaus, Appl. Phys. Lett., 75, 2438 (1999).

[7]. G. Chen, S. Q. Zhou, D.-Y. Yao, C. J. Kim, X. Y. Zheng, Z. L. Liu and K. L. Wang, Proceedings of the 17th International Conference on Thermoelectrics, 202 (1998).

[8]. A. Shakouri and J. E. Bowers, Appl. Phys. Lett., 71, 1234 (1997).

[9]. A. Shakouri, C. Labounty, P. Abraham, J. Piprek, and J. E. Bowers, Material Research Society Symposium Proceedings, 545, 449 (1999).

[10]. L. W. Whitlow and T. Hirano, J. Appl. Phys., 78, 5460 (1995).

[11]. C. B. Vining, J. Appl. Phys., 69, 331 (1991).

[12]. S.-M Lee, D. G. Cahill and R. Venkatasubramanian, Appl. Phys. Lett., 70, 2957 (1997).